



Numerical analysis of heat transfer in fish containers

Steinar Geirdal Snorrason



Faculty of Industrial Engineering, Mechanical Engineering and
Computer Science
University of Iceland
2014

NUMERICAL ANALYSIS OF HEAT TRANSFER IN FISH CONTAINERS

Steinar Geirdal Snorrason

60 ECTS thesis submitted in partial fulfillment of a
Magister Scientiae degree in Mechanical Engineering

Advisors

Dr. Halldór Pálsson, Associate Professor, University of Iceland
Sigurjón Arason MSc, Professor, University of Iceland, Matís
Dr. Björn Margeirsson, Research Manager, Promens Dalvik/Tempra

Faculty Representative
Sveinn Víkingur Árnason

Faculty of Industrial Engineering, Mechanical Engineering and
Computer Science
School of Engineering and Natural Sciences
University of Iceland
Reykjavik, May 2014

Numerical analysis of heat transfer in fish containers

60 ECTS thesis submitted in partial fulfillment of a M.Sc. degree in Mechanical Engineering

Copyright © 2014 Steinar Geirdal Snorrason

All rights reserved

Faculty of Industrial Engineering, Mechanical Engineering and Computer Science

School of Engineering and Natural Sciences

University of Iceland

VRII, Hjardarhagi 2-6

107, Reykjavik, Reykjavik

Iceland

Telephone: 525 4000

Bibliographic information:

Steinar Geirdal Snorrason, 2014, Numerical analysis of heat transfer in fish containers, M.Sc. thesis, Faculty of Industrial Engineering, Mechanical Engineering and Computer Science, University of Iceland.

Printing: Háskólaprent, Fálkagata 2, 107 Reykjavík

Reykjavik, Iceland, May 2014

Abstract

Insulated packaging can play an important role in protecting perishable foods against temperature abuse at different stages of the chill chain. This thesis is aimed at developing and validating three-dimensional time dependent heat transfer models of fish packed in five types of insulated containers under temperature-abusive conditions. All of the containers under consideration were without lid. Results show that there is a low overall mean absolute error as well as a low Δ remaining shelf life (RSL) at 0°C (the difference of the RSL between simulation and experiment) in all simulations when compared to the experimental results which implies a good agreement between the simulated and experimental results. This demonstrates that numerical heat transfer modelling can be used to cost effectively predict temperature changes in food packed in insulated containers.

Útdráttur

Einangraðar pakkningar geta skipt sköpum í verndun á matvælum sem eiga í hættu með að skemmast undir hitaálagi. Markmið þessarar ritgerðar er að þróa og sannreyna þrívíddar tímaháð varmaflutnings módel fyrir fisk pakkaðan í fimm mismunandi fiskiker undir hitaálagi. Öll kerin sem notuð voru höfðu enginn lok. Niðurstöðurnar sýna að það er lág heildarskekkja ásamt lágum heildarmismun af eftirlifandi geymslutíma þegar tilraunaniðurstöður voru bornar saman við niðurstöður úr módelinu. Þetta sýnir gott samræmi milli tilraunar og hermun. Þetta sýnir að hermun varmaflutnings getur verið notað á ódýran hátt til að meta hitabreytingar í einangruðum pakkningum sem innihalda matvæli.

Contents

List of Figures	ix
List of Tables	xiii
Nomenclature	xv
Acknowledgments	xvii
1. Introduction	1
2. Background	3
2.1. Fishing containers	3
2.1.1. Materials	4
2.2. Whitefish	5
2.3. Heat transfer modelling	8
3. Materials and methods	11
3.1. Instruments	11
3.1.1. Temperature data loggers	11
3.1.2. Heat flow meter	12
3.2. Measurements	13
3.2.1. Properties of fish containers	13
3.2.2. Thermal load trials	15
3.3. Numerical heat transfer model	18
3.3.1. Thermal properties of whitefish	19
3.3.2. Boundary conditions	19
3.3.3. Initial conditions	20
4. Results	21
4.1. Thermal properties of fish containers	21
4.2. 660L PUR Container	23
4.3. 460L PUR Container	26
4.4. 660L PE Container	29
4.5. 460L PE Container	32
4.6. 340L PE Container	35

5. Discussion	39
6. Conclusion	41
Bibliography	43
A. RRS result figures	49
A.1. 660L PUR Container	49
A.2. 460L PUR Container	51
A.3. 660L PE Container	52
A.4. 460L PE Container	55
A.5. 340L PE Container	56

List of Figures

2.1. Apparent specific heat for a material with gradual phase change (see ASHRAE (2006)).	6
3.1. FOX300 heat flow meter open with a sample inside.	12
3.2. 30×30 cm PE sample.	13
3.3. PE sample where skin has been removed, seen from above.	14
3.4. PE sample where skin has been removed, seen from the side.	14
3.5. Positions of temperature sensors inside the containers containing saithe backbones under thermal load.	15
3.6. Vertical cross section A shown in Figure 3.5.	16
3.7. Vertical cross section B shown in Figure 3.5.	16
3.8. 660 L PUR and PE containers containing saithe backbones.	17
3.9. Mesh used in 660 L PUR/PE model.	18
4.1. Measured thermal conductivity of a) PUR foam, b) PE foam and c) PE skin.	21
4.2. Measured thermal conductivity with regard to thickness of a) PUR foam, b) PE foam and c) PE skin.	22
4.3. Temperature evolution at different positions (see Figures 3.7 and 3.6) inside a 660 L PUR container containing saithe backbones under thermal load.	23

LIST OF FIGURES

4.4. Comparison between simulation results and experimental results for 5 positions at; a) bottom center, b) bottom corner, c) mid center, d) in wall, e) top corner (see Figures 3.7 and 3.6) and f) ambient temperature.	24
4.5. Temperature evolution at different positions (see Figures 3.7 and 3.6) inside a 460 L PUR container containing saithe backbones under thermal load.	26
4.6. Comparison between simulation results and experimental results for 5 positions at; a) bottom center, b) bottom corner, c) mid center, d) in wall, e) top center (see Figures 3.7 and 3.6) and f) ambient temperature.	27
4.7. Temperature evolution at different positions (see Figures 3.7 and 3.6) inside a 660 L PE container containing saithe backbones under thermal load.	29
4.8. Comparison between simulation results and experimental results for 5 positions at; a) bottom center, b) bottom corner, c) mid center, d) in wall, e) top center (see Figures 3.7 and 3.6) and f) ambient temperature.	30
4.9. Temperature evolution at different positions (see Figures 3.7 and 3.6) inside a 460 L PE container containing saithe backbones under thermal load.	32
4.10. Comparison between simulation results and experimental results for 5 positions at; a) mid center, b) in wall, c) top center, d) top corner (see Figures 3.7 and 3.6) and e) ambient temperature.	33
4.11. Temperature evolution at different positions (see Figures 3.7 and 3.6) inside a 340 L PE container containing saithe backbones under thermal load.	35
4.12. Comparison between simulation results and experimental results for 5 positions at; a) bottom center, b) bottom corner, c) mid center, d) top center, e) top corner (see Figures 3.7 and 3.6) and f) ambient temperature.	36
A.1. RRS results at bottom corner in 660 L PUR container.	49
A.2. RRS results at bottom center in 660 L PUR container.	50

A.3. RRS results at mid center in 660 L PUR container.	50
A.4. RRS results at bottom corner in 460 L PUR container.	51
A.5. RRS results at bottom center in 460 L PUR container.	51
A.6. RRS results at mid center in 460 L PUR container.	52
A.7. RRS results at top center in 460 L PUR container.	52
A.8. RRS results at bottom corner in 660 L PE container.	53
A.9. RRS results at bottom center in 660 L PE container.	53
A.10. RRS results at mid center in 660 L PE container.	54
A.11. RRS results at top center in 660 L PE container.	54
A.12. RRS results at mid center in 460 L PE container.	55
A.13. RRS results at top corner in 460 L PE container.	55
A.14. RRS results at top center in 460 L PE container.	56
A.15. RRS results at bottom corner in 340 L PE container.	56
A.16. RRS results at bottom center in 340 L PE container.	57
A.17. RRS results at mid center in 340 L PE container.	57
A.18. RRS results at top corner in 340 L PE container.	58
A.19. RRS results at top center in 340 L PE container.	58

List of Tables

2.1. Known values of density, heat conductivity and specific heat capacity for PUR foam ^a , PE skin ^b and PE foam ^c	5
3.1. Specification of temperature data loggers.	11
4.1. Measured properties of PUR, PE skin and PE foam.	22
4.2. Mean absolute error of simulated results for four data loggers in the 660 L PUR container.	24
4.3. RSL of saithe backbones in 660 L PUR containers.	25
4.4. Mean absolute error of simulated results for four data loggers in the 460 L PUR container.	27
4.5. RSL of saithe backbones in 660 L PUR containers.	28
4.6. Mean absolute error of simulated results for four data loggers in the 660 L PE container.	30
4.7. RSL of saithe backbones in 660 L PE containers.	31
4.8. Mean absolute error of simulated results for four data loggers in the 460 L PE container.	33
4.9. RSL of saithe backbones in 460 L PE containers.	34
4.10. Mean absolute error of simulated results for four data loggers in the 340 L PE container.	36
4.11. RSL of saithe backbones in 340 L PE containers.	37

LIST OF TABLES

5.1. Comparison of the simulated and experimental results.	39
--	----

Nomenclature

BCo	bottom corner of container
BCe	bottom center of container
c_p	specific heat capacity, $\text{kJ kg}^{-1}\text{K}^{-1}$
EPS	expanded polystyrene
FPR	fibre-reinforced plastic
HDPE	high-density polyethylene
k	thermal conductivity, $\text{W m}^{-1}\text{K}^{-1}$
MC	mid height center of container
PE	polyethylene
PUR	polyurethane
RH	relative humidity, %
RSL	remaining self life
TCo	top corner of container
TCe	top center of container
w	water content, %
ρ	density, kg m^{-3}

Acknowledgments

This work was supported by AVS R&D Fund of Ministry of Fisheries in Iceland (project no. S13 018-13), the Akureyri region growth agreement and Promens. The financial support is gratefully acknowledged. I would also like to thank HB Grandi for providing the fish used in the experiments and giving access to their facilities. I would like to express my gratitude to my advisors Björn Margeirsson, Halldór Pálsson and Sigurjón Arason. I would also like to thank my family and friends for their support during the work on the thesis.

1. Introduction

Temperature has to be considered when looking at the quality and safety of fresh food, such as fish, beef and poultry. If temperature control in fresh food supply chains is inadequate it will inevitably cause quality deterioration, decreased product safety, more product waste and depreciated product value. The relative loss of perishable foods through a lack of refrigeration has been estimated as 20% worldwide and as high as 9% for developed countries (IIR, 2009). This indicates that optimization of temperature control in the fresh food supply chain can improve overall quality. The fresh food temperature during transport and storage in the chill chain is affected by different factors, such as the food temperature during packaging, thermal properties of the foodstuff, interaction of ambient conditions (e.g. temperature, air flow, solar radiation, humidity) and time.

Insulated packaging can play an important role in protecting the perishables against temperature abuse. Considerable emphasis has been put on studying the insulating properties of wholesale boxes designed for 3-13 kg of fresh food (Froese, 1998; Burgess, 1999; Choi and Burgess, 2007; Gospavic et al., 2012; Margeirsson et al., 2011, 2012a,b,c; Navaranjan et al., 2013). However, the thermal insulation of double-walled plastic containers, designed for around 300–500 kg of fresh food, has not been studied as extensively even though the ambient thermal load on the plastic containers can be just as severe as on the wholesale boxes. Numerical heat transfer modelling has been shown to be a valuable tool to cost effectively predict whitefish temperature changes under thermal load (Margeirsson et al., 2011, 2012b,c). It has even been used to improve the design of a commercial expanded polystyrene (EPS) box type, with capacities of 3–7 kg, with regard to thermal insulation (Valtýsdóttir et al., 2011) resulting in new box types, which are the most popular in their size category in Iceland.

1. Introduction

The aim of the thesis is to develop and validate three-dimensional time dependent heat transfer models of fish in five types of fish containers without lids under temperature-abusive conditions. The models should be able to predict the spatio-temporal temperature evolution, with a minimum overall mean error of 2 °C, inside each container under different ambient conditions, which is a common request from the users of fish containers.

2. Background

2.1. Fishing containers

Fishing containers exist in different sizes and materials from simple baskets of woven reeds, bamboo, cane or grasses, to containers made from wood, metals and plastics. These containers are typically used for the transport of ice and fish. In order to reduce the melting of ice and therefore the heating of fish being transported, insulation materials may be used when the containers are manufactured. Use of any particular type of container depends very much on the local economic situation and fishery being pursued (Pizzali and Shawyer, 2003).

The containers are mainly used to perform the following functions: (Brox et al., 1984)

1. Ease the handling of small and large quantities of fish.
2. Simplify and increase the speed of unloading/loading and transportation of raw material.
3. Protect the fish against physical damage contamination and other deteriorating factors.
4. Offer a suitable packing unit for fish and ice.
5. Contain the fish under such conditions that it reaches the buyer in the best possible condition.
6. Help to protect the raw material against natural deteriorating effects.
7. Help to make maximum utilization of resources and to achieve optimum economical results through the whole system of handling from harvest to consumption.

As mentioned before, containers of various types, sizes and of different materi-

2. Background

als are used all over the world to hold fish both on board vessels, in processing, during transport and under general storage. In the whole system of correct fish handling the container is only one factor in the process. Knowledge of handling, necessary regulations/laws and the specific behavior of fish meat under various conditions are also important points to consider. Poor handling and lack of suitable containers leads to as much as 20-30% spoilage in many countries (Brox et al., 1984). Where the major loss in quality and value are occurring between harvesting operations and first sale in landing areas. It is envisaged that with the increased availability and wider use of properly designed containers for use on small fishing vessels will reduce wastage of fresh fish in small-scale fisheries (Pizzali and Shawyer, 2003).

There are a number of factors that limit the achievement of this goal. These include the relatively high cost of ready-made insulated containers that are for the most part manufactured in industrialized countries and need to be imported. Fishermen tend to use the locally made containers rather than the plastic or metal imported containers due to the extra cost that is involved. However as the fishery becomes more developed more emphasis has to be put on the product quality and the need for better containers increases (Pizzali and Shawyer, 2003).

Containers and their different materials have limitations. Therefore is it important to choose the right container system at the right time and to use it in accordance with laid down objectives (Brox et al., 1984).

2.1.1. Materials

Common materials used for the manufacture of insulated containers are fibre-reinforced plastic (FRP) and high-density polyethylene (HDPE) often with plastic foams for insulation (Pizzali and Shawyer, 2003).

Double-walled HDPE containers that are constructed in a single piece using a rotational moulding process are one of the most common type of insulated container that is used in fisheries. The HDPE walls are in the range of 3 to 6 mm and the total thickness differs according to the design parameters such as size and capacity of the container. The HDPE double-walled containers are considered to be superior to those manufactured with other materials since they are able to withstand relatively rough handling compared to FPR, that tends to be more brittle and prone to impact damage and fractures (Pizzali and Shawyer, 2003).

HDPE insulated containers can have, when handled correctly, a lifespan of about five to seven years. There can be a problem repairing HDPE containers when broken but medium-density polyethylene is more repairable via welding. HDPE containers can be used in a temperature range of up to 100 °C and down to -40 °C.

However it is not recommended to work with the HDPE at the lower range since it becomes brittle and is therefore not very suitable for use in frozen fish stores. HDPE containers are commercially available in the range of 50 L in capacity up to 1100 L and the thermal efficiency differs according to the intended use and design (Pizzali and Shawyer, 2003).

One of the best commercially available choices of insulation material is polyurethane (PUR) foam. It has good thermal insulating properties, low moisture-vapour permeability, high resistance to water absorption, and relatively high mechanical strength and low density. In addition, it is relatively easy and economical to install. Polyethylene (PE) foam has similar properties to PUR foam. (Pizzali and Shawyer, 2003).

Known properties of PUR foam , PE skin and PE foam are listed in Table 2.1

Table 2.1: Known values of density, heat conductivity and specific heat capacity for PUR foam^a, PE skin^b and PE foam^c.

Material	ρ [kg m ⁻³]	k [W m ⁻¹ K ⁻¹]	c_p [kJ kg ⁻¹ K ⁻¹]
PUR foam	30	0.026	1.5
PE foam	70	0.05	2.3
PE skin	930	0.44	1.64

^a See BING (2006)

^b See Martienssen (2005)

^c See ISO/FDIS 10456 (2007)

2.2. Whitefish

Thermal properties

Fish has no sharply defined phase change region and that can, in general, when modelling a phase change cause complications in numerical heat transfer modelling (Pham, 1995; Hardarson, 1996; Pham, 2006). For problems solved with fixed grid methods, such as apparent heat capacity methods, the complications can be related to the sharp peak in the apparent heat capacity of the food (Figure 2.1), which is due to the latent heat.

The water content of food has a great influence on its thermophysical properties. The different water content of whitefish depending on the season (Huss, 1995) causes certain variability in the thermophysical properties of the raw material and

2. Background

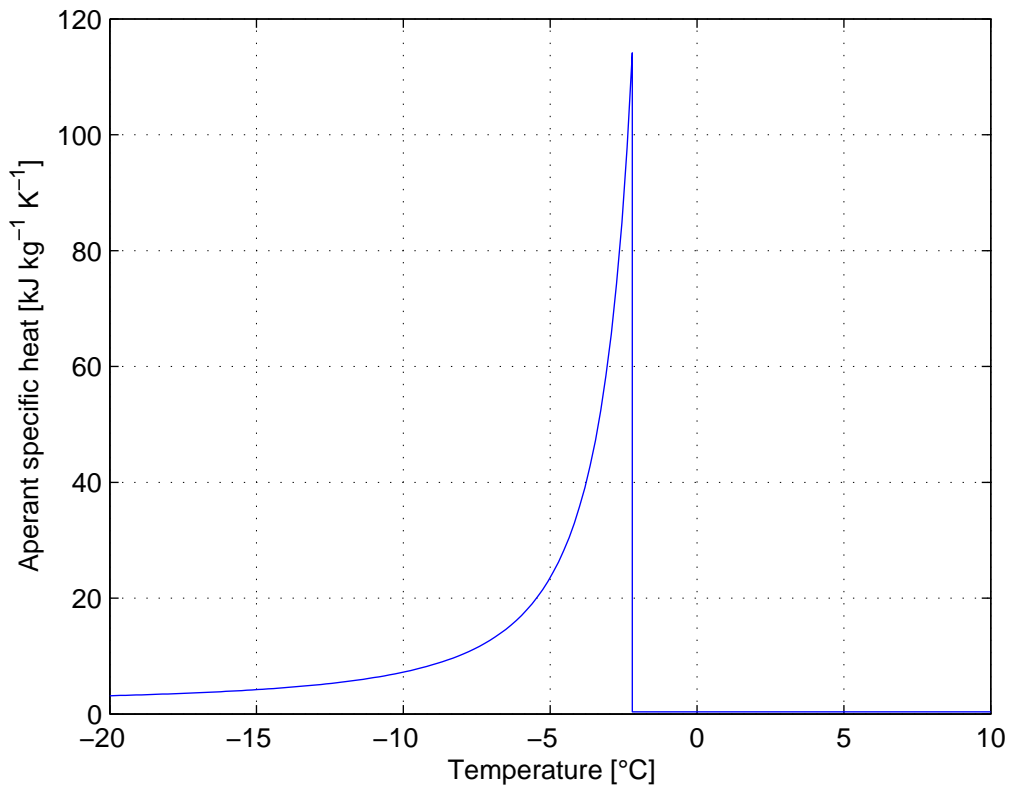


Figure 2.1: Apparent specific heat for a material with gradual phase change (see ASHRAE (2006)).

the resulting fish products. The water content (w) of cod can range from 78 to 83% (Murray and Burt, 2001).

The ability to predict thermophysical properties in foodstuff is difficult and two approaches can yield different results. For example the attempt to estimate the thermal conductivity (k) of cod Sweat (1986) gives values between 0.40 and 0.43 Wm⁻¹K⁻¹ and on the other hand Miles et al. (1983) yields values between 0.30 and 0.50 Wm⁻¹K⁻¹.

Models for relative rate of spoilage

Spoilage of fish starts as soon as the fish dies and is the result of a whole series of complicated changes brought about in the dead fish by its own enzymes, by chemical action and by bacteria. In addition to bacterial and enzymatic changes, chemical changes involving oxygen from the air can produce rancid odours and flavours. Thus, spoilage is a natural process once the fish dies, but chilling can slow down this process and prolong the shelf life of fish (Graham et al., 2004).

Temperature has a great effect on both the enzymatic and microbiological activity. However if the temperature range is from 0 to 25°C, microbiological activity has a greater effect (Huss, 1995).

For fresh seafood, the relative rate of spoilage (RRS) at a given temperature has been defined as the shelf life at 0°C divided by the shelf life at a given temperature (Dalgaard, 2002). For fresh fish 0°C is used as a reference temperature but using different reference temperatures like 5°C can be appropriate for lightly preserved seafood. Mathematical RRS models are developed on the basis of shelf life data obtained at different storage temperatures in experiments where shelf life is determined by sensory evaluation. RSS models can be valid for a wide range of storage temperatures since they do not take into account the types of reactions that cause spoilage at different temperatures. RSS-models are simple but still most useful for calculation of shelf life at different storage temperatures. (DTU Aqua, 2009)

It has been shown that different combinations of time and temperature have an additive effect of shelf life in fresh fish (Charm et al., 1972; McMeekin et al., 1988). This was confirmed with vacuum-packed cold-smoked salmon (Dalgaard et al., 2004).

Different RRS-models are required to evaluate the effect of temperature during storage of different kinds of seafood. Therefore, Seafood Spoilage & Safety Predictor (SSSP) includes models for fresh seafood, lightly preserved seafood and models with user defined-parameter values that can be applied for any type of food (DTU Aqua, 2009).

Types of RRS-models

SSSP includes three different models. The exponential spoilage model with the temperature characteristic 'a'. The Arrhenius spoilage model with the temperature characteristic 'Ea' is also called the apparent activation energy. Finally there is the square-root spoilage model with the temperature characteristic ' T_{min} ' (Eqn. 2.1) that is used in this thesis. When RRS models are developed, rates of spoilage (RS, days⁻¹) can be calculated as the reciprocal of the shelf life determined by sensory evaluation. Log-transformed RS-data then can be fitted to the exponential spoilage model and to the the Arrhenius model whereas square-root transformed RS data are fitted to the square-root spoilage model (Eqn. 2.1) (DTU Aqua, 2009).

In the following equations T is temperature in °C, k is a constant and T_{min} is the temperature characteristics in the model.

2. Background

square-root model:

$$\sqrt{RS} = k \times (T - T_{min}) \quad (2.1)$$

After estimation of temperature characteristics with Eqn. 2.1 shelf life can be predicted at different temperatures using Eqn. 2.2.

square-root RSS model:

$$\text{shelf life at } T^{\circ}\text{C} = \frac{\text{shelf life at } T_{ref}}{\left(\frac{T - T_{min}}{T_{ref} - T_{min}}\right)^2} \quad (2.2)$$

RRS models are developed on the basis of shelf life data obtained directly from storage trials with naturally contaminated seafood.

2.3. Heat transfer modelling

The effects of temperature abuse on refrigerated food and product temperature changes to abusive ambient conditions and thermal properties of the food and packaging solutions have been studied extensively. Single packages and in pallet loads exposed to thermal load have been both tested with experimental and numerical methods to show that the temperature distribution is in general inhomogeneous, with highest temperatures at the corners of the packages/loads and the most stable temperatures at their centre (Dolan et al., 1987; Almonacid-Merino et al., 1993; Moureh and Derens, 2000; Moureh et al., 2002; Tanner et al., 2002b; Stubbs et al., 2004; Laguerre et al., 2008).

A three-dimensional Computational fluid dynamics (CFD) model using the CFD software PHOENICS was developed by Moureh and Derens (2000) to predict temperature increase in pallet loads of frozen fish under thermal load. The numerical results were validated by performing experiments with pallets loaded with 11 levels of frozen fish packages (height: 14 cm) both on a shaded dock in February (at 4°C, 80% RH) and on an open dock in July (at 21.6°C ° C, 50% RH). The product temperatures were –25 °C and –20 °C in February and July. Temperature-recording sensors were placed at strategic locations to best map the temperature evolution. The experimental and numerical results showed both that the greatest temperature rise was at the top level and the model predicted a rise over 25 min of 2.7 °C and 6.4 °C in the February and July simulations (Moureh and Derens, 2000). This is

in conjunction with a study on temperature changes of cut flowers during flight (Sillekens et al., 1997) and a study on land based transport of poultry (Raab et al., 2008).

According to the ATP (2010) a brief temperature rise at the surface of frozen fish above the maximum allowed temperature of -18°C is limited to 3°C . In the study of Moureh and Derens (2000) the temperature rise in the summer is 3.4°C too high and comes close in the winter situation. Fresh fish is more sensitive to temperature fluctuations than frozen fish and thus, even more emphasis should be put on minimizing temperature fluctuations of the fresh product.

A numerical heat transfer model of chilled cheese packaged in an EPS box under thermal load was developed to study temperature distribution (Stubbs et al., 2004). Inside the EPS box gel refrigerant was applied at different surfaces (top, bottom, and sides). Distributing the cooling capacity of the gel refrigerant was, as would be expected, beneficial with regard to minimizing product temperature rise.

More recently a study by East and Smale (2008) and East et al. (2009) on how zone based heat transfer modelling (based on Tanner et al. (2002a,b)) could be combined with a genetic algorithm in order to optimize the design of a thermally insulated box with regard to cost. Additionally Laguerre et al. (2008) developed a a temperature-predictive mode where chilled products and a refrigerant (referred to as phase change material) were loaded into a insulated box. At a given position the product temperature evolution was assumed to be a linear response of the initial temperature of the load and the ambient temperature. The main heat transfer mechanism was considered to be conduction due to the small air space above the product and that would not allow for significant natural convection. The results showed that the model was applicable for both constant and variable ambient temperature as long as the PCM was not completely melted.

Margeirsson et al. (2011, 2012b,c) used ANSYS FLUENT to redesign a 5 kg EPS box. In order to do this the authors looked at transport in air. What they discovered was that there can be a product temperature difference up to 10.5°C in non-superchilled fresh fish pallet load. As well as the storage life difference between the most and the least sensitive boxes on a full size pallet in a real air transport chain can exceed 1-1.5 days. The boxes that were used were EPS boxes design with sharp corners. The redesign rounded of the corners in order to minimize the heat rise of the fish.

None of the aforementioned studies covered a numerical heat transfer model of fresh fish in double walled foam insulated containers but that is the main subject of this thesis.

3. Materials and methods

3.1. Instruments

3.1.1. Temperature data loggers

The specification of the different temperature sensors used is presented in Table 3.1. CO 03.01 wireless temperature sensors from Controlant (Reykjavík, Iceland), that are developed for Promens, were used to monitor all product temperatures and some ambient temperatures, which were also measured with Tidbit v2 temperature loggers from Onset Computer Corporation (Bourne, MA, USA).

Table 3.1: Specification of temperature data loggers.

Device	Resolution	Range	Accuracy
CO 03.01	0.0625 °C	−30 to 80 °C	± 0.5 °C ^a at −20 to 40 °C
Tidbit v2	0.02 °C	−20 to 70 °C	± 0.2 °C at 0 to 50 °C

^a equal to the allowed deviation from the set point by standards for food distribution (BS EN 12830, 1999).

3. Materials and methods

3.1.2. Heat flow meter

In order to maximize the accuracy of the numerical heat transfer models, the heat conductivity was measured with FOX300 heat flow meter (LaserComp, Saugus, Massachusetts, USA), The heat flow meter can be seen in Figure 3.1.

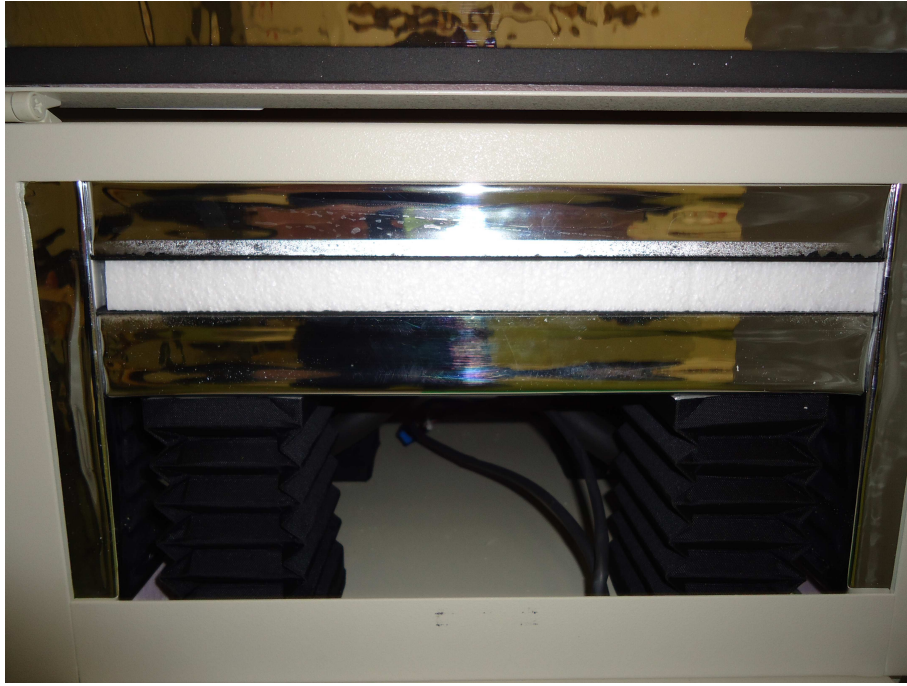


Figure 3.1: FOX300 heat flow meter open with a sample inside.

3.2. Measurements

3.2.1. Properties of fish containers

Due to variances in their manufacturing process, the observed thermal properties of fish containers can vary from the nominal values. In order to maximize the accuracy of the numerical heat transfer models, the heat conductivity and density of different fish container types were measured. The heat flow meter was calibrated so that the upper plate is held at a constant temperature of 20 °C and the lower plate at a constant temperature of 0 °C this means that the mean temperature difference between the plates is 10 °C and a ΔT of 20 °C. The dimensions of the samples were around 30×30 cm (area) and the thickness in the range 20–40 mm.

The measured samples consisted of a polyethylene shell insulated with foamed polyurethane (PUR container) or foamed polyethylene (PE containers). The samples from the PUR containers were measured with the skin attached to the foam yielding the overall thermal conductivity and density of the sample. Because the PE samples were of such a poor quality the core had to be cut out and the foam measured on its own. For the PUR samples the PE skin was removed and the thermal conductivity and density of the foam core were measured. The samples can be seen in Figures 3.2, 3.3 and 3.4



Figure 3.2: 30×30 cm PE sample.

3. Materials and methods



Figure 3.3: PE sample where skin has been removed, seen from above.



Figure 3.4: PE sample where skin has been removed, seen from the side.

The bulk density of all materials was calculated by measuring the thickness and area, weighing the samples and dividing the weight by the calculated volume.

3.2.2. Thermal load trials

During the experiments saithe (*Pollachius virens*) backbones were used as the food-stuff because they have similar thermal properties as cod and were easily available. The PUR and PE containers were tested in the same trial, meaning that these container types got a very similar thermal load. Temperature data loggers were placed at five different locations within the food (saithe backbones) and one was integrated in the container wall. These locations can be seen in Figures 3.5–3.7.

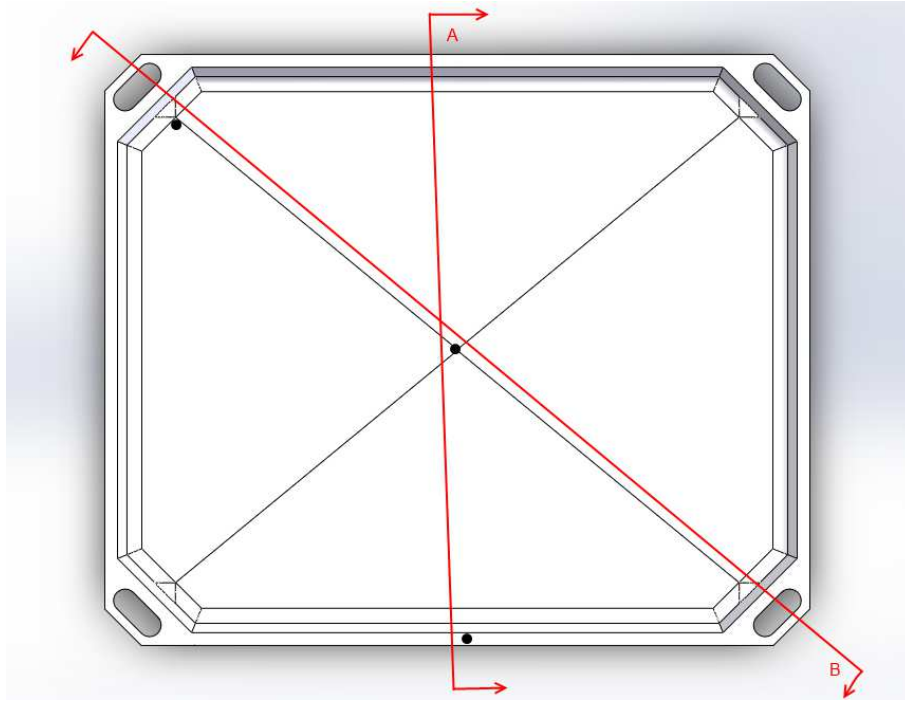


Figure 3.5: Positions of temperature sensors inside the containers containing saithe backbones under thermal load.

3. Materials and methods

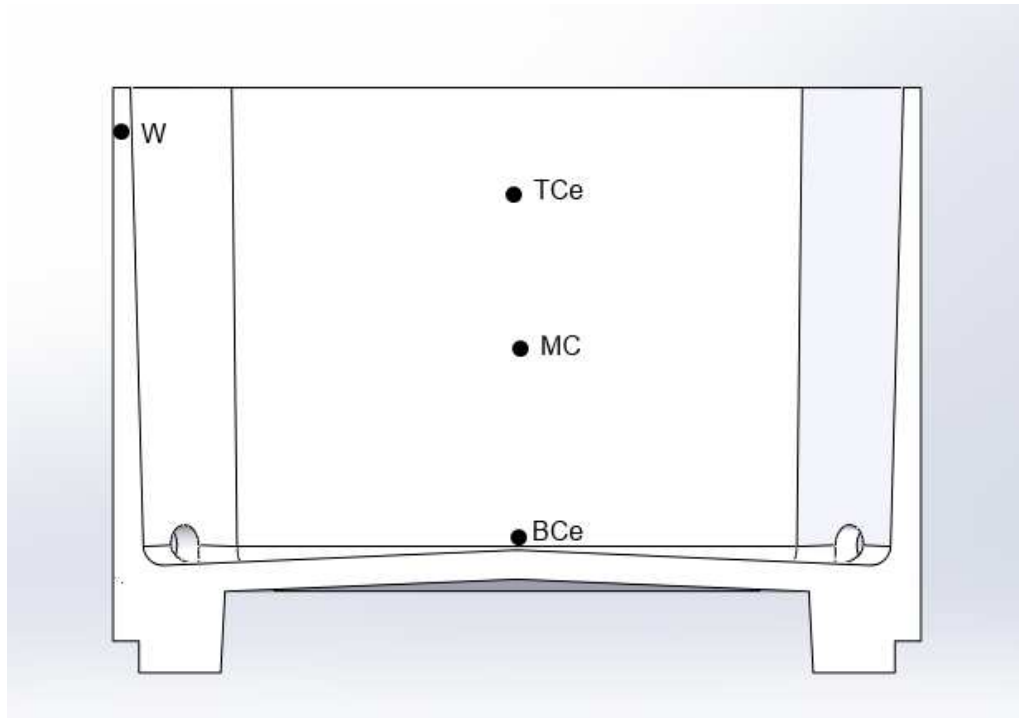


Figure 3.6: Vertical cross section A shown in Figure 3.5.

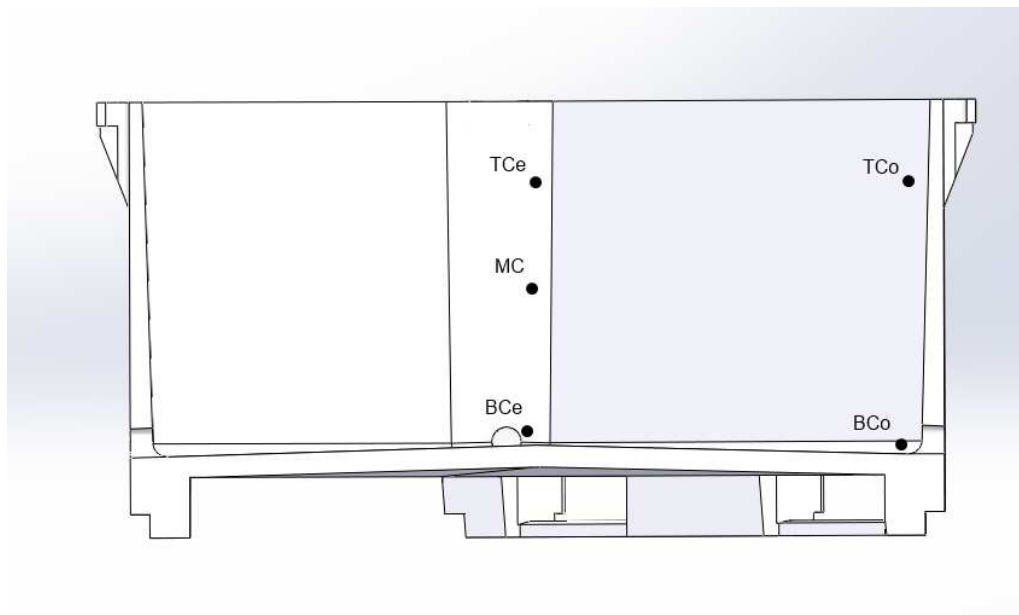


Figure 3.7: Vertical cross section B shown in Figure 3.5.

In Figure 3.8 the 660 L containers can be seen filled with the saithe backbones.



Figure 3.8: 660 L PUR and PE containers containing saithe backbones.

The containers were kept in a chilled storage room for 40 h at 2 °C, then moved to 10 °C for 24 h and then put back into the chilled storage room for 10 h.

3.3. Numerical heat transfer model

Three-dimensional finite volume heat transfer models were developed using the Computational Fluid Dynamics (CFD) software FLUENT for the following containers containing fish under temperature-abusive conditions:

- PUR containers
 - 660 L
 - 460 L
- PE containers
 - 660 L
 - 460 L
 - 340 L

All cases are time dependent where the ambient temperature changes with time. The models contain fish backbones that is filled up according to the measured weight. In Figure 3.9 the computational mesh of the PUR 660L container can be seen.

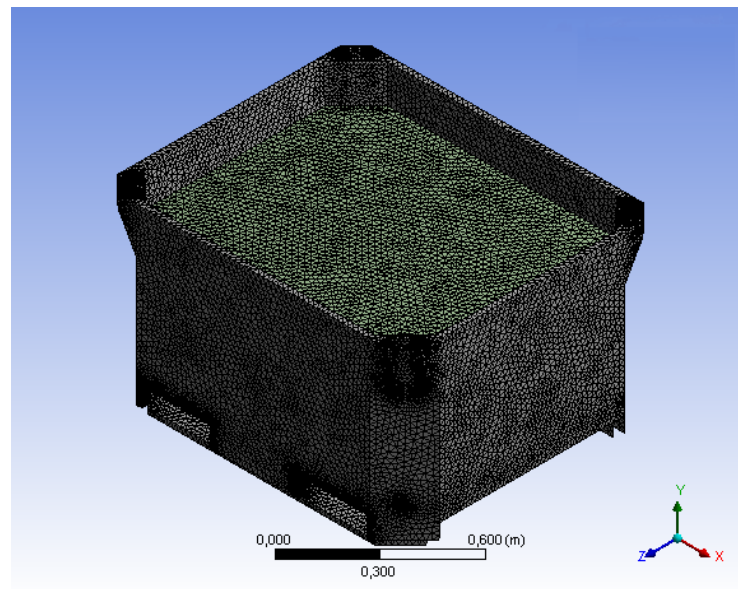


Figure 3.9: Mesh used in 660 L PUR/PE model.

In all cases, inside the fish mass, heat is transferred only by conduction.

3.3.1. Thermal properties of whitefish

In the models the following fixed thermal properties are adopted:

- $\rho = 1018 \text{ m}^{-3}$ (see Zueco et al. (2004))
- $c_p = 3.50 \text{ kJ kg}^{-1} \text{ K}^{-1}$ (mean value between 4 and 32 °C, see Rao and Rizvi (1995))
- $k = 0.50 \text{ W m}^{-1} \text{ K}^{-1}$ (see Jowitt et al. (1983))

The density (ρ), specific heat (c_p) and thermal conductivity (k) are slightly different than in the literature. That is because the fish backbones are mixed with water which should increase the conductivity and decrease the density as compared to fish.

3.3.2. Boundary conditions

Mixed convection and external radiation boundary conditions are applied to the sides, top and bottom of the fish containers. Equations 3.1 - 3.3 show how the convection was calculated (Holman, 2002).

- Fish: top of fish (horizontal plane):

$$h_{conv,top} = 1.32 \left(\frac{\Delta T}{x} \right)^{1/4} \quad (3.1)$$

- container bottom (horizontal plane):

$$h_{conv,bottom} = 0.59 \left(\frac{\Delta T}{x} \right)^{1/4} \quad (3.2)$$

3. Materials and methods

- container sides (vertical plane):

$$h_{conv,sides} = 1.42 \left(\frac{\Delta T}{x} \right)^{1/4} \quad (3.3)$$

Where $\Delta T = T_{amb} - T_{w,out}$ ($T_{w,out}$: outside fish container wall temperature) and x is characteristic length.

Emissivity of 0.9 is adopted for the fish containers and the fish according to The Engineering Toolbox (2013) and Holman (2002).

In PUR and PE the container walls are pure PUR/PE rigid foam and the PE skin is added by using thermal contact resistance.

3.3.3. Initial conditions

In all the heat transfer models developed the mean fish temperatures are obtained from the temperature data loggers and are used to define uniform initial conditions throughout the whole computational domain. Linear interpolation is used in order to make the data as realistic as possible. Since the data loggers were not spread over the entire container as is seen in Figures 3.5–3.7 it was estimated that the initial temperature was symmetrical. This is a simplification of the real conditions because in the experiments this may not be the case.

4. Results

4.1. Thermal properties of fish containers

The material measurements can be seen in Figure 4.1. The PUR foam samples have got some variability that is due to the fact that the skin was roughly removed. It has however low thermal conductivity. The PE foam has very low variability and this is due to the fact that the sample was cut out. The PE skin has a very high variability, higher than the measured average. This could be due to limitations in the heat flow meter.

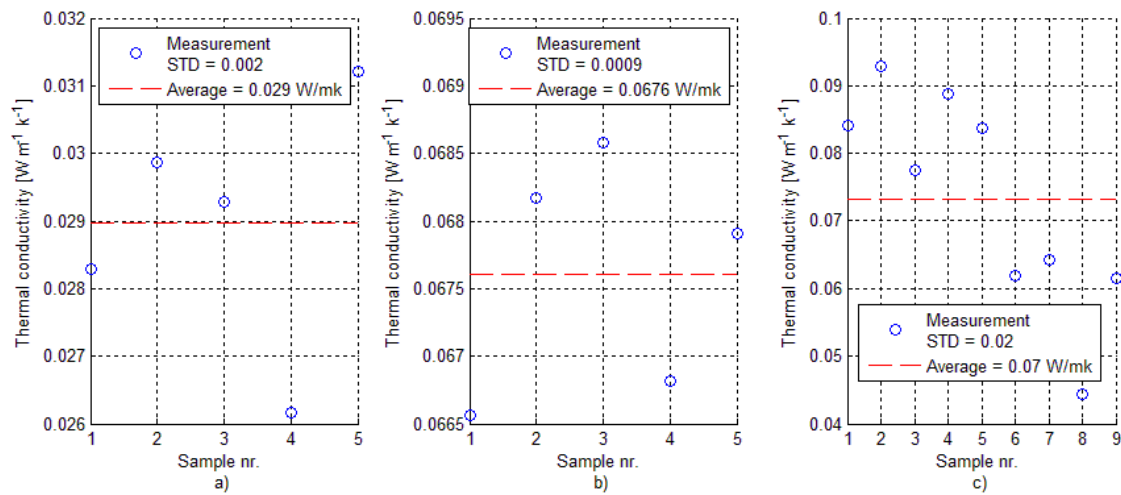


Figure 4.1: Measured thermal conductivity of a) PUR foam, b) PE foam and c) PE skin.

4. Results

The results from the measurements of thermal properties of fish containers are summarized in table 4.1.

Table 4.1: Measured properties of PUR, PE skin and PE foam.

Material	ρ [kg m ⁻³]	k [W m ⁻¹ K ⁻¹]
PUR foam	64 ± 19	0.029 ± 0.002
PE foam	143 ± 3	0.068 ± 0.001
PE skin	840 ± 60	0.07 ± 0.02

To test the limitations of the heat flow meter the thermal conductivity was studied in relation to the sample thickness as can be seen in Figure 4.2. There is no conjunction between the sample thickness and the thermal conductivity in PUR foam and PE foam. The PE skin however shows a clear conjunction between the sample thickness and the thermal conductivity. Therefore the measured data could not be used in the calculations and the known value ($0.44 \text{ W m}^{-1}\text{K}^{-1}$) was used.

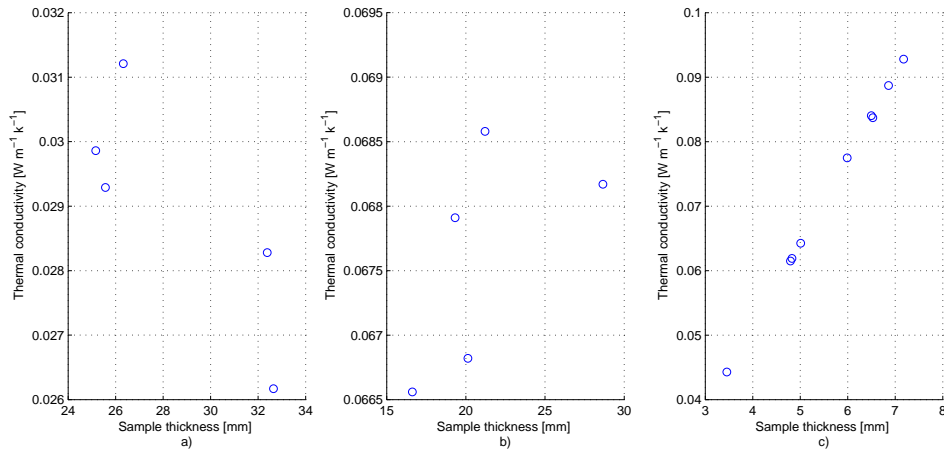


Figure 4.2: Measured thermal conductivity with regard to thickness of a) PUR foam, b) PE foam and c) PE skin.

4.2. 660L PUR Container

The results from the temperature measurements for the 660 L PUR containers are presented in Figure 4.3.

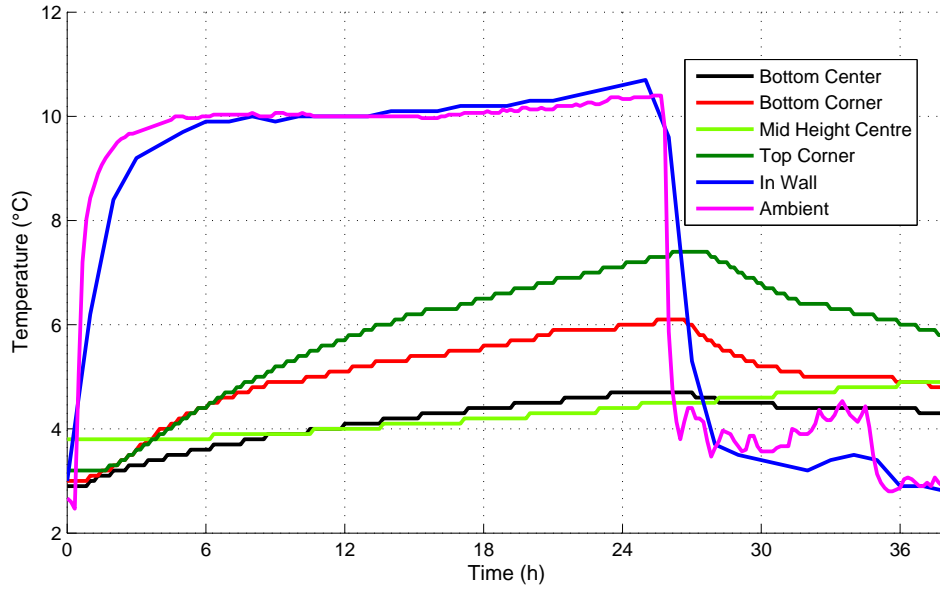


Figure 4.3: Temperature evolution at different positions (see Figures 3.7 and 3.6) inside a 660 L PUR container containing saithe backbones under thermal load.

4. Results

In Figure 4.4 the simulation results and experimental results for the 660 L PUR container are compared.

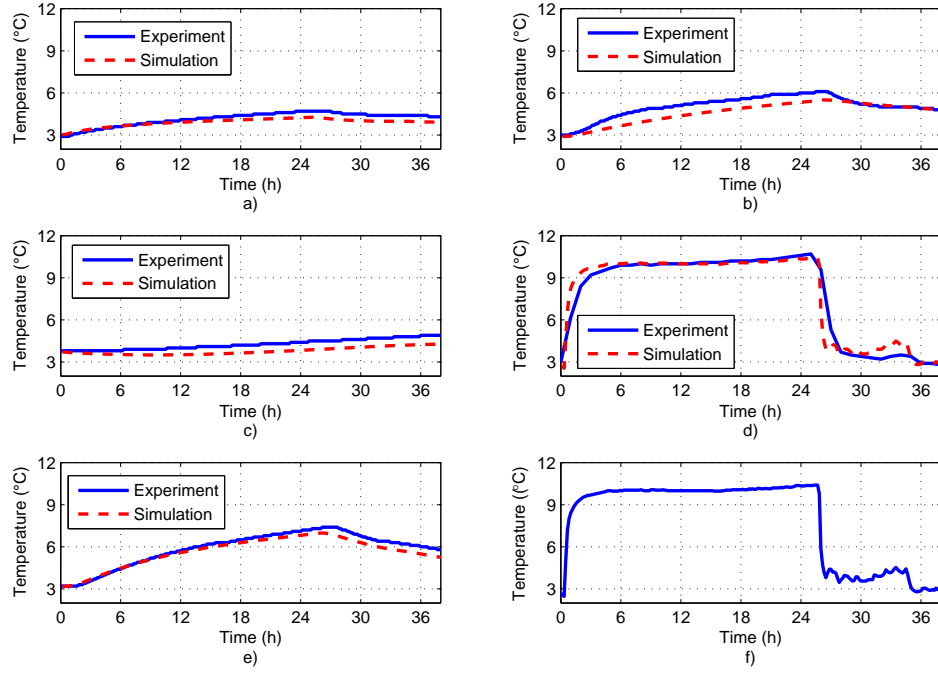


Figure 4.4: Comparison between simulation results and experimental results for 5 positions at; a) bottom center, b) bottom corner, c) mid center, d) in wall, e) top corner (see Figures 3.7 and 3.6) and f) ambient temperature.

The heat transfer model underestimates the heat transfer at most of the positions and in Table 4.2 the mean absolute error is shown.

Table 4.2: Mean absolute error of simulated results for four data loggers in the 660 L PUR container.

Position	Mean absolute error [°C]
BCo	0.5
BCe	0.3
MC	0.5
TCo	0.3

That gives a total mean absolute error of 0.4 °C.

Spoilage

In table 4.3 the RSL difference between the experimental and the simulated results, after having been loaded into the RRS model, at the end of the trial can be seen. The full results are shown in figure form in Appendix A

Table 4.3: RSL of saithe backbones in 660 L PUR containers.

Position	Δ RSL at 0 °C [days]	Δ RSL at 5 °C [days]	Δ RSL at 10 °C [days]
BCo	0.19	0.08	0.05
BCe	0.09	0.04	0.02
MC	0.08	0.04	0.02
TCo	0.1	0.05	0.03

4.3. 460L PUR Container

The results from the temperature measurements for the 460 L PUR containers are presented in Figure 4.5.

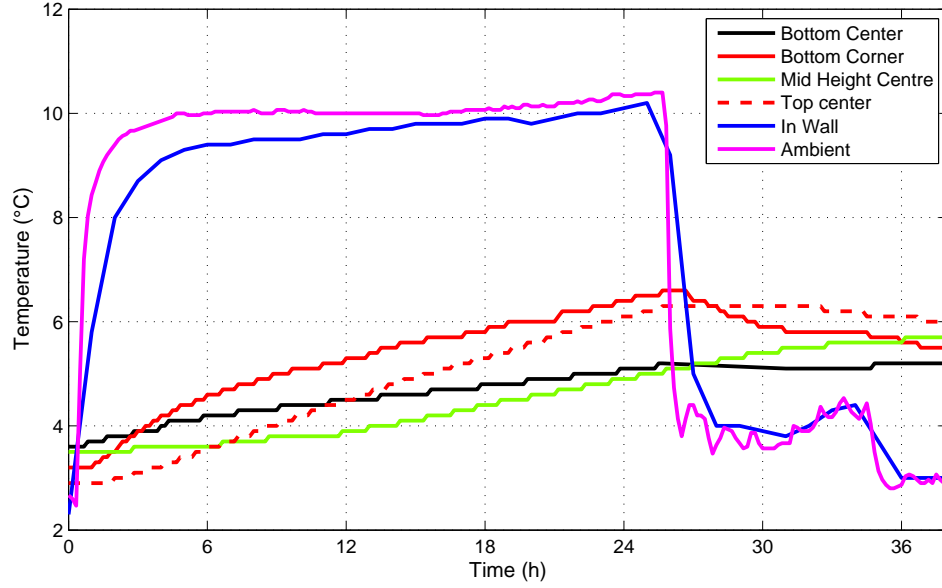


Figure 4.5: Temperature evolution at different positions (see Figures 3.7 and 3.6) inside a 460 L PUR container containing saithe backbones under thermal load.

In Figure 4.6 the simulation results and experimental results for the 460 L PUR container are compared.

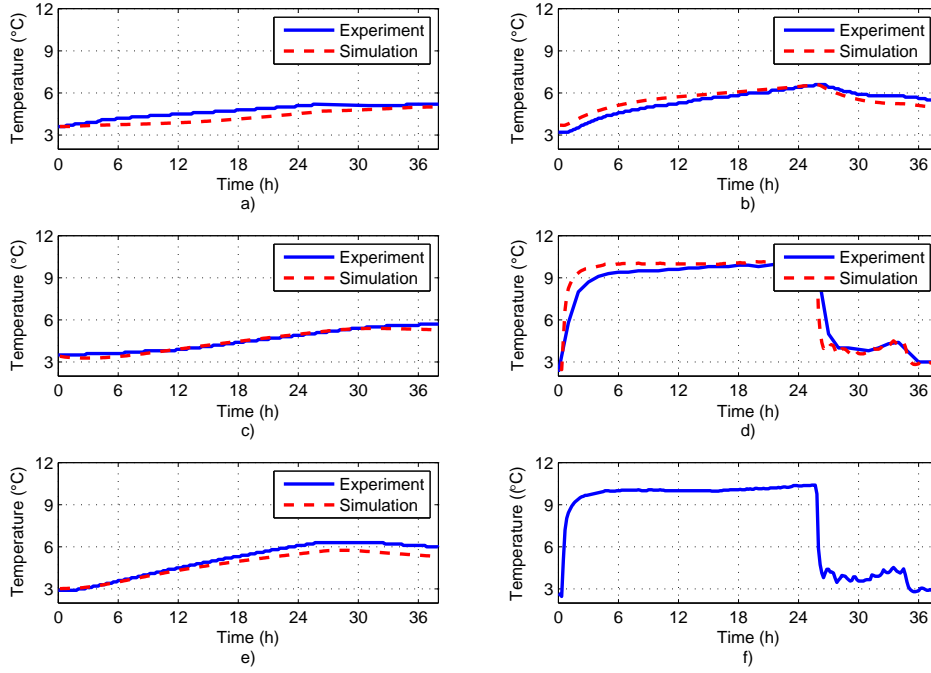


Figure 4.6: Comparison between simulation results and experimental results for 5 positions at; a) bottom center, b) bottom corner, c) mid center, d) in wall, e) top center (see Figures 3.7 and 3.6) and f) ambient temperature.

The heat transfer model underestimates the heat transfer at most of the positions and in Table 4.4 the mean absolute error is shown.

Table 4.4: Mean absolute error of simulated results for four data loggers in the 460 L PUR container.

Position	Mean absolute error [°C]
BCo	0.4
BCe	0.4
MC	0.1
TCe	0.4

That gives a total mean absolute error of 0.3 °C.

4. Results

Spoilage

In table 4.5 the RSL difference between the experimental and the simulated results, after having been loaded into the RRS model, at the end of the trial can be seen. The full results are shown in figure form in Appendix A

Table 4.5: RSL of saithe backbones in 660 L PUR containers.

Position	Δ RSL at 0 °C [days]	Δ RSL at 5 °C [days]	Δ RSL at 10 °C [days]
BCo	0.06	0.03	0.02
BCe	0.12	0.08	0.05
MC	0.02	0.01	0.005
TCe	0.17	0.07	0.04

4.4. 660L PE Container

The results from the temperature measurements for the 660 L PE containers are presented in Figure 4.7.

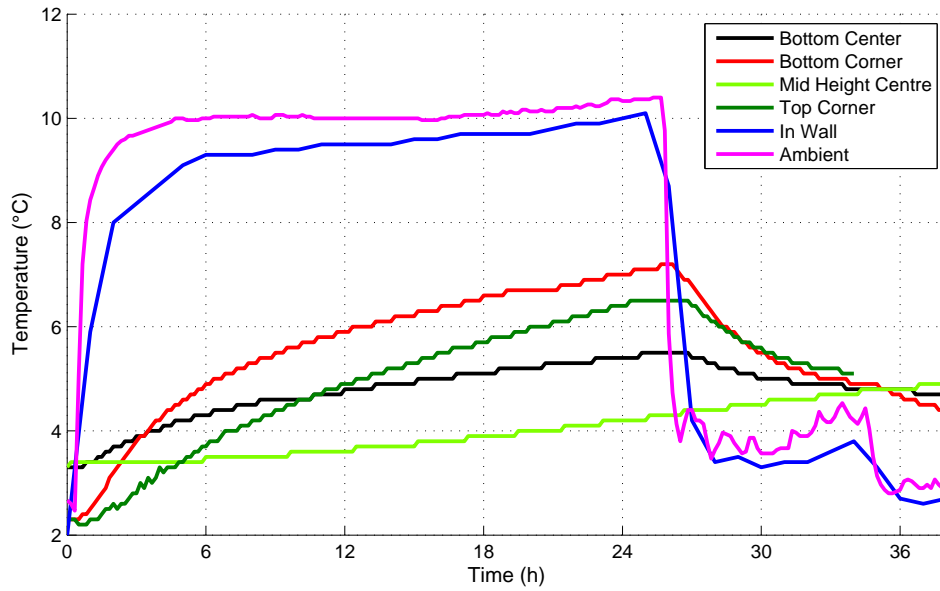


Figure 4.7: Temperature evolution at different positions (see Figures 3.7 and 3.6) inside a 660 L PE container containing saithe backbones under thermal load.

4. Results

In Figure 4.8 the simulation results and experimental results for the PE container are compared.

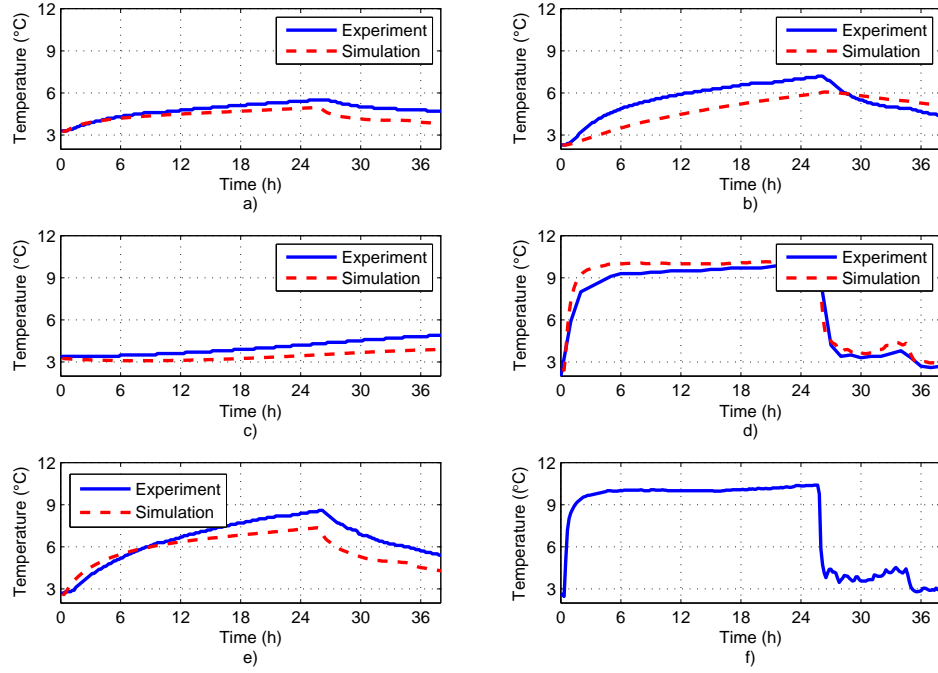


Figure 4.8: Comparison between simulation results and experimental results for 5 positions at; a) bottom center, b) bottom corner, c) mid center, d) in wall, e) top center (see Figures 3.7 and 3.6) and f) ambient temperature.

The heat transfer model underestimates the heat transfer at most of the positions and in Table 4.6 the mean absolute error is shown.

Table 4.6: Mean absolute error of simulated results for four data loggers in the 660 L PE container.

Position	Mean absolute error [°C]
BCo	0.9
BCe	0.5
MC	0.6
TCe	0.9

That gives a total mean absolute error of 0.7°C.

Spoilage

In table 4.7 the RSL difference between the experimental and the simulated results, after having been loaded into the RRS model, at the end of the trial can be seen. The full results are shown in figure form in Appendix A

Table 4.7: RSL of saithe backbones in 660 L PE containers.

Position	Δ RSL at 0 °C [days]	Δ RSL at 5 °C [days]	Δ RSL at 10 °C [days]
BCo	0.34	0.15	0.08
BCe	0.21	0.09	0.05
MC	0.27	0.12	0.07
TCe	0.33	0.15	0.08

4.5. 460L PE Container

The results from the temperature measurements for the 460 L PE containers are presented in Figure 4.9.

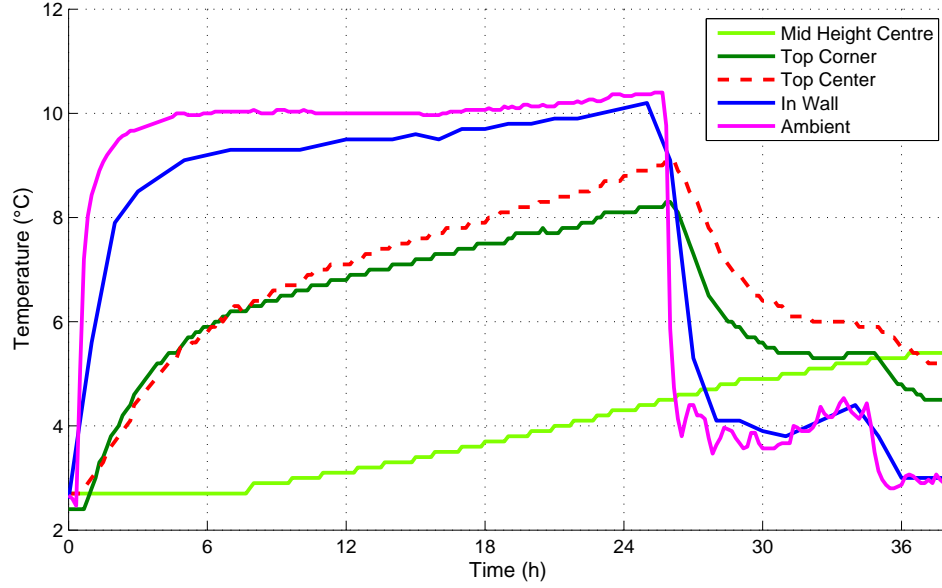


Figure 4.9: Temperature evolution at different positions (see Figures 3.7 and 3.6) inside a 460 L PE container containing saithe backbones under thermal load.

In Figure 4.10 the simulation results and experimental results for the PE container are compared.

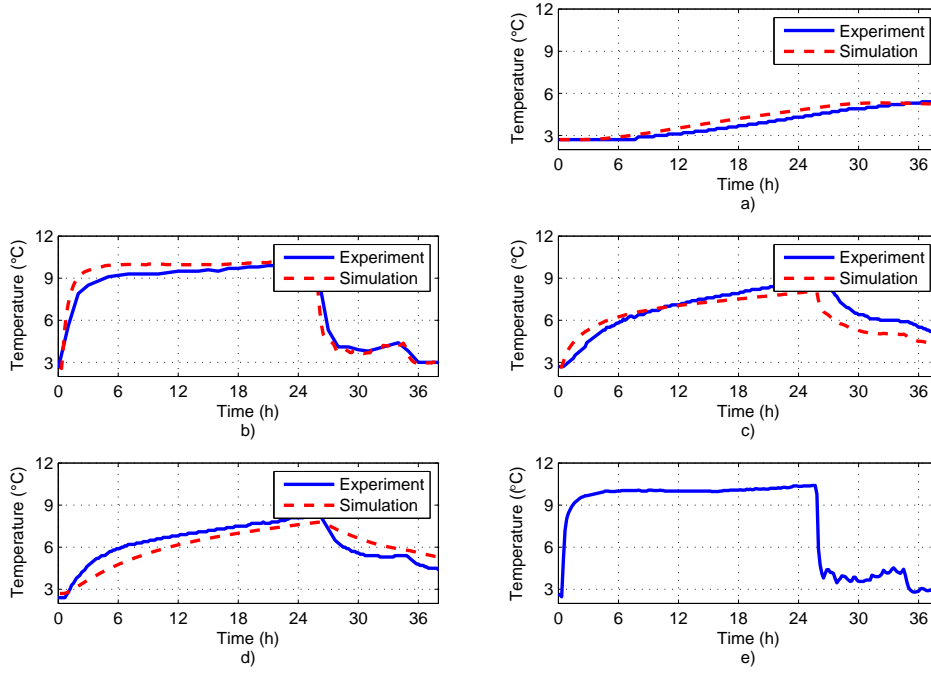


Figure 4.10: Comparison between simulation results and experimental results for 5 positions at; a) mid center, b) in wall, c) top center, d) top corner (see Figures 3.7 and 3.6) and e) ambient temperature.

The heat transfer model underestimates the heat transfer at most of the positions. When looking at the bottom corner in the experiment the temperature rises faster then in the simulation. This could be because the temperature logger has shifted and moved to the plug area where blood water resides. In the top corner the temperature in the experiment behaves differently than in the simulation this could be due the sensor shifting during the experiment. In Table 4.8 the mean absolute error is shown.

Table 4.8: Mean absolute error of simulated results for four data loggers in the 460 L PE container.

Position	Mean absolute error [°C]
MC	0.3
TCo	0.3
TCe	0.7

That gives a total mean absolute error of 0.6 °C.

4. Results

Spoilage

In table 4.9 the RSL difference between the experimental and the simulated results, after having been loaded into the RRS model, at the end of the trial can be seen. The full results are shown in figure form in Appendix A

Table 4.9: RSL of saithe backbones in 460 L PE containers.

Position	Δ RSL at 0 °C [days]	Δ RSL at 5 °C [days]	Δ RSL at 10 °C [days]
MC	0.15	0.07	0.04
TCo	0.09	0.04	0.02
TCe	0.24	0.11	0.06

4.6. 340L PE Container

The results from the temperature measurements for the 340 L PE containers are presented in Figure 4.11.

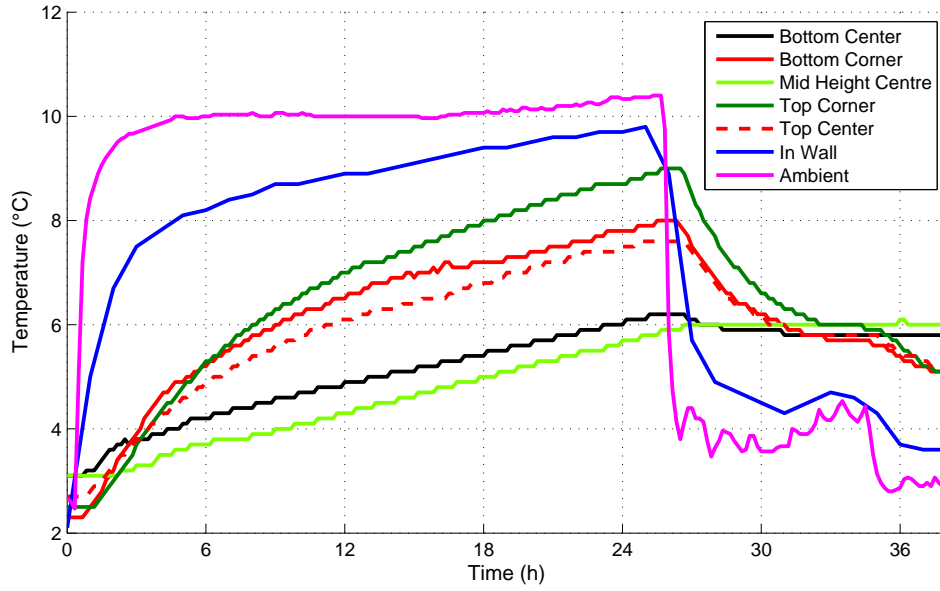


Figure 4.11: Temperature evolution at different positions (see Figures 3.7 and 3.6) inside a 340 L PE container containing saithe backbones under thermal load.

4. Results

In Figure 4.12 the simulation results and experimental results for the PE container are compared.

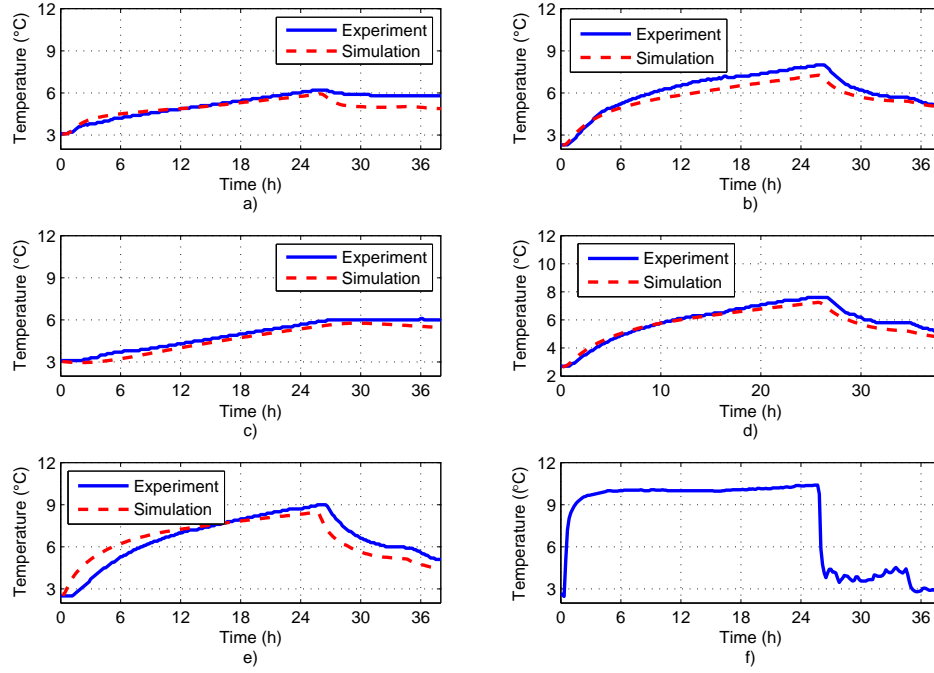


Figure 4.12: Comparison between simulation results and experimental results for 5 positions at; a) bottom center, b) bottom corner, c) mid center, d) top center, e) top corner (see Figures 3.7 and 3.6) and f) ambient temperature.

The heat transfer model underestimates the heat transfer at most of the positions and in Table 4.10 the mean absolute error is shown.

Table 4.10: Mean absolute error of simulated results for four data loggers in the 340 L PE container.

Position	Mean absolute error [°C]
BCo	0.5
BCe	0.2
MC	0.3
TCo	0.7
TCe	0.3

That gives a total mean absolute error of 0.4 °C.

Spoilage

In table 4.11 the RSL difference between the experimental and the simulated results, after having been loaded into the RRS model, at the end of the trial can be seen. The full results are shown in figure form in Appendix A

Table 4.11: RSL of saithe backbones in 340 L PE containers.

Position	Δ RSL at 0 °C [days]	Δ RSL at 5 °C [days]	Δ RSL at 10 °C [days]
BCo	0.24	0.11	0.06
BCe	0.23	0.10	0.06
MC	0.34	0.15	0.09
TCO	0.27	0.12	0.07
TCe	0.19	0.08	0.05

5. Discussion

Of the two insulating materials PUR foam is a better insulator than PE foam having a heat transfer coefficient of $0.029 \text{ W m}^{-1}\text{K}^{-1}$ vs. $0.067 \text{ W m}^{-1}\text{K}^{-1}$ for the PE foam. These values are similar to the theoretical values. After looking at the results of the PE skin that gave $0.07 \text{ W m}^{-1}\text{K}^{-1}$ with STD of $0.02 \text{ W m}^{-1}\text{K}^{-1}$ that is a really high STD and thus the thermal conductivity was studied in relation to the sample thickness to test the limitations of the heat flow meter. The results show no relation in PE foam and PUR foam. However in the PE skin samples there is a clear relation. This is probably due to the fact that the samples are not completely smooth and the thinner the sample is the air that is between the sample and the device has a greater effect. For this reason the known value for PE skin was used in the calculations or $0.44 \text{ W m}^{-1}\text{K}^{-1}$. The density ($\rho [\text{kg m}^{-3}]$) that was measured was in good relation to known data.

In Table 5.1 an overall comparison of the simulated and the experimental results can be seen. It can be seen that the Maximum error ranges from 0.5 to 0.9°C and the mean error ranges from 0.3 to 0.7°C . Furthermore the maximum ΔRSL ranges from 0.19 to 0.34 days. All this reinforces that the simulated results fit well to the experimental results for all the simulations.

Table 5.1: Comparison of the simulated and experimental results.

Container	Maximum error [$^\circ\text{C}$]	Mean error [$^\circ\text{C}$]	maximum ΔRSL [days]
660L PUR	0.5	0.4	0.19
460L PUR	0.4	0.3	0.12
660L PE	0.9	0.7	0.34
460L PE	0.7	0.6	0.24
340L PE	0.7	0.4	0.34

Here the containers will be compared both different materials in the same size as well as different sizes in same material. When looking at 660L PUR vs. the 660L PE the temperature rise in the PUR container. The temperature rise in the PE container is greater than in the PUR container which confirms the results from the heat flow meter. The same can be said for the 460L PUR vs. the 460L PE containers. When comparing different sizes the larger containers (660L) have a lower

5. Discussion

heat rise then the smaller ones 460 L and 340 L. This is due to the fact that the larger container has more mass to heat up and therefore takes longer.

6. Conclusion

Three-dimensional finite volume heat transfer models have been developed for fish packed in five container types without lids under temperature-abusive conditions. The heat transfer models were validated with experimental results, which revealed heterogeneous temperature distributions within the fish containers under thermal load of around 10 °C for 24 h. Both the experimental and simulation results indicate that the temperature evolution at the position, which is currently used for wireless MIND ID/temperature sensors in some Promens containers, is much closer to the ambient temperature evolution than the temperature evolution within the food. Judging from the low overall mean absolute errors of the models (between 0.3 and 0.7 °C) and the low Δ RSL at 0 °C (between 0.12 and 0.34 days), a good agreement between simulated and experimental results was obtained. This supports the fact that numerical heat transfer modelling can be used to cost effectively predict temperature changes in food packed in insulated containers.

Bibliography

- Almonacid-Merino, S.F., Torres, A.J., 1993. Mathematical models to evaluate temperature abuse effects during distribution of refrigerated solid foods. *Journal of Food Engineering* Vol. 20, pp. 223-245
- American Society of Heating, Refrigerating and Air-Conditioning Engineers (2006). 2006 ASHRAE handbook refrigeration. American Society of Heating, Refrigeration and Air-Conditioning Engineers.
- BS EN 12830, 1999. Temperature recorders for the transport, storage and distribution of chilled, frozen, deep-frozen/quick-frozen food and ice cream.
- BING (2006). Thermal insulation materials made of rigid polyurethane foam (PUR/PIR). Federation of European Rigid Polyurethane Foam Associations, volume number 1. Retrieved from http://www.excellence-in-insulation.eu/site/fileadmin/user_upload/PDF/library/reports/BING_TECH_REP_on_Thermal_insulation_materials_made_of_rigid_polyurethane_foam.pdf
- Brox, J., Kristiansen, M., Myrseth, A., Aasheim, P.W. 1984. Planning and engineering data. 4. Containers for fish handling. *FAO Fish.Circ.*, (773):53 p. ., Rome, Italy. Retrieved from <http://www.fao.org/docrep/003/r1263e/r1263e00.htm>
- Burgess, G., 1999. Practical thermal resistance and ice requirement calculations for insulating packages. *Packaging Technology and Science* Vol. 12, pp. 75–80.
- Charm, S.E., Learson, R.J., Ronsivalli, L.J., Schwartz, M. 1972. Organoleptic technique predicts refrigeration shelf life of fish. *Food Technol.*Vol. 26, pp. 65-68.
- Choi, S., Burgess, G., 2007. Practical Mathematical Model to Predict the Performance of Insulating Packages. *Packaging Technology and Science* Vol. 20, pp. 369–380.
- Dalgaard, P. 2002. Modelling and predicting the shelf life of seafood. In *Safety and Quality Issues in Fish Processing*(H.A. BREMNER, ed.) pp.191–219, Woodhead Publishing Ltd, London, U.K
- Dalgaard, P, Murillo, E.I., Jørgensen, L.V. 2004. Modelling the effect of temperature on shelf life and on the interaction between the spoilage microflora and *Listeria monocytogenes* in cold-smoked salmon. Chapter 22 In: Shahidi, F. and

BIBLIOGRAPHY

- Simpson, B. K. (eds), Seafood Quality and Safety. Advances in the new millennium. ScienceTech Publishing Company, St. John's, Newfoundland, Canada, pp. 281-302.
- Dolan, K.D., Singh, R. P., Heldman, D.R., 1987. Prediction of Temperature in Frozen Foods Exposed to Solar Radiation. J. Food Process. Preserv., Volp 11, pp. 135-158.
- DTU Aqua, 2009. Seafood Spoilage and Safety Predictor (SSSP) ver. 3.1, National Institute of Aquatic Resources (DTU Aqua), Technical University of Denmark (DTU) retrived from http://sssp.dtuaqua.dk/HTML_Pages/Help/English/Index.htm
- East, A.R., Smale, N.J., 2008. Combining a hybrid genetic algorithm and a heat transfer model to optimise an insulated box for use in the transport of perishables. Vol. 26,pp. 1322-1334.
- East, A., Smale, N., Kang, S., 2009. A method for quantitative risk assessment of temperature control in insulated boxes. International Journal of Refrigeration Vol. 32, pp. 1505-1513.
- Froese, R., 1998. Insulating properties of styrofoam boxes used for transporting live fish. Aquaculture Vol. 159, pp. 283-292.
- Gospavic, R., Margeirsson, B., Popov, V. 2012. Mathematical model for estimation of the three-dimensional unsteady temperature variation in chilled packaging. International Journal of Refrigeration Vol. 35, pp.1304—1317.
- Graham, J., Johnston, W.A., Nicholson, F.J. 1992. Ice in Fisheries FAO Fisheries Technical Paper. No. 331. Rome, FAO. 75p. Retrieved from http://innri.unuftp.is/short_courses/safety_qm_srilanka06/Additional%20material/Ice%20in%20fisheries_FA0.pdf
- Harðarson, V., 1996. Thermo-physical properties of food and their significance on freezing tunnel design. PhD thesis (in Norwegian). Norwegian University of Science and Technology, Trondheim, Norway.
- Holman, J., 2002. Heat transfer, 9th ed. McGraw-Hill, New York, USA.
- Huss, H.H., 1995. Quality and Quality Changes in Fresh Fish. FAO Fish. Techn. Paper 348. FAO, Rome, Italy
- IIR, 2009. The Role of Refrigeration in Worldwide Nutrition - 5th IIR Informatory Note on Refrigeration and Food. International Institute of Refrigeration, Paris, France.

- ISO/FDIS, (2007). ISO/FDIS 10456:2007 Building materials and products - Hygrothermal properties - Tabulated design values and procedures for determining declared and design thermal values Geneva, Switzerland: ISO/FDIS.
- Jowitt, R., Escher, F., Hallström, B., Meffert, H.F.T., Spiess, W.E.L, Vos, G., 1983. Physical properties of Foods. Applied Science Publishers, Essex, England.
- Laguerre, O., Ben Aissa, M.F., Flick, D., 2008. Methodology of temperature prediction in an insulated container equipped with PCM. *International Journal of Refrigeration* Vol. 31, pp. 1063-1072.
- Margeirsson, B., Gospavic, R., Pálsson, H., Arason, S., Popov, V. 2011. Experimental and numerical modelling comparison of thermal performance of expanded polystyrene and corrugated plastic packaging for fresh fish. *International Journal of Refrigeration* Vol. 34, pp. 573—585.
- Margeirsson, B., Lauzon, H.L., Pálsson, H., Popov, V., Gospavic, R., Jónsson, M.P., Sigurgísladóttir, S., Arason, S. 2012a. Temperature fluctuations and quality deterioration of chilled cod (*Gadus morhua*) fillets packaged in different boxes stored on pallets under dynamic temperature conditions. *International Journal of Refrigeration* Vol. 35, pp. 187—201.
- Margeirsson, B., Pálsson, H., Gospavic, R., Popov, V., Jónsson, M.P., Arason, S. 2012b. Numerical modelling of temperature fluctuations of chilled and super-chilled cod fillets packaged in expanded polystyrene boxes stored on pallets under dynamic temperature conditions. *Journal of Food Engineering* 113(1):87—99.
- Margeirsson, B., Pálsson, H., Popov, V., Gospavic, R., Arason, S., Sveinsdóttir, K., Jónsson, M.P. 2012c. Numerical modelling of temperature fluctuations in super-chilled fish loins packaged in expanded polystyrene and stored at dynamic temperature conditions. *International Journal of Refrigeration* Vol. 35, pp. 1318—1326.
- Martienssen, W., & Warlimont, H. (2005). Springer handbook of condensed matter and materials data. Springer, Heidelberg, New York.
- McMeekin, T.A., Olley, J. and Ratkowsky, D.A. 1988. Temperature effects on bacterial growth rates. In: Bazin, M.J. and Prosser, J.I. (Eds.) *Physiological Models in Microbiology*, pp. 75-89. Boca Raton, Florida: CRC Press, Inc.
- Miles, C.A., Van Beek, G., Veerkamp, C.H., 1983. Calculation of Thermophysical Properties of Foods, in: Jowitt, R., Escher, F., Hallström, B., Meffert, H.F.T., Spiess, W.E.L, Vos, G. (Eds.), *Physical properties of Foods*. Applied Science Publishers, Essex, England, pp. 269-312.
- Moureh, J., Derens, E., 2000. Numerical modelling of the temperature increase in frozen food packaged in pallets in the distribution chain. *International Journal of Refrigeration* Vol. 23, pp. 540-552

BIBLIOGRAPHY

- Moureh, J., Laguerre, O., Flick, D., Commere, B., 2002. Analysis of use of insulating pallet covers for shipping heat-sensitive foodstuffs in ambient conditions. *Computers and Electronics in Agriculture* Vol. 34, pp. 89-1
- Murray, J., Burt, J.R., 2001. The Composition of Fish - Torry advisory note no. 38. Torry research station in partnership with FAO and SIFAR. Aberdeen, Scotland. Retrieved from <http://www.fao.org/wairdocs/tan/x5916e/x5916e00.htm>
- Navaranjan, N., Fletcher, G.C., Summers, G., Parr, R., Anderson, R. 2013. Thermal insulation requirements and new cardboard packaging for chilled seafood exports. *Journal of Food Engineering* Vol. 119, pp. 395—403.
- Pham, Q.T., 1995. Comparison of General Purpose Finite Element Methods for the Stefan Problem. *Numerical Heat Transfer Part B-Fundamentals* Vol. 27, pp. 417-435.
- Pham, Q.T., 2006. Modelling heat and mass transfer in frozen foods: a review. *International Journal Refrigeration* Vol. 29, pp. 876-888.
- Pizzali, A.F.M., Shawyer, M. 2003. The use of ice on small fishing vessels. FAO Fish. Techn. Paper 436, FAO, Rome, Italy. Retrieved from <http://www.fao.org/docrep/006/y5013e/y5013e00.htm>
- Raab, V., Bruckner, S., Beierle, E., Kampmann, Y., Petersen, B., Kreyenschmidt, J., 2008. Generic model for the prediction of remaining shelf life in support of cold chain management in pork and poultry supply chains. *Journal on Chain and Network Science* Vol. 8, pp. 59-73.
- Rao, M., Rizvi, S., 1995. *Engineering Properties of Foods*, 2nd ed. Marcel Decker, Inc., New York, USA.
- Sillekens, J.J.M., Oskam, N.A., Ceton, C., 1997. Validated models of the thermodynamic behaviour of perishables during flight. In: *Modelling of thermal properties and behaviour of foods during production, storage and distribution*, June 23-25, 1997. Prague, Czech Republic.
- Stubbs, D.M., Pulko, S.H., Wilkinson, A.J., 2004. Wrapping strategies for temperature control of chilled foodstuffs during transport. *Transactions of the Institute of Measurement and Control* Vol. 26, pp. 69-80.
- Sweat, V.E., 1986. Thermal properties of foods, in: Rao, M., Rizvi, S. (Eds.), *Engineering Properties of Foods*. Marcel Decker, Inc., New York, USA, pp. 49-87.
- Tanner, D.J., Cleland, A.C., Opara, L.U., Robertson, T.R., 2002a. A generalised mathematical modelling methodology for design of horticultural food packages exposed to refrigerated conditions: part 1, formulation. *International Journal of Refrigeration* Vol. 25, pp. 33-42.

- Tanner, D.J., Cleland, A.C., Opara, L.U., 2002b. A generalised mathematical modelling methodology for design of horticultural food packages exposed to refrigerated conditions: part 2, heat transfer modelling and testing. *International Journal of Refrigeration* Vol. 25, pp. 43-53.
- The Engineering Toolbox, 2013. Emissivity coefficients of some common materials. Retrieved from http://www.engineeringtoolbox.com/emissivitycoefficients-d_447.html [accessed November 21, 2013].
- United Nations Economic Commission for Europe, 2010. Agreement Transport Perishables, Agreement on the international carriage of perishable foodstuffs and on the special equipment to be used for such carriage. Available at <http://www.unece.org/trans/main/wp11/atp.html> [accessed December 2, 2013].
- Valtýsdóttir, K.L., Margeirsson, B., Arason, S., Pálsson, H., Gospavic, R., Popov, V., 2011a. Numerical Heat Transfer Modelling for Improving Thermal Protection of Fish Packaging. In: CIGR Section VI International Symposium on Towards a Sustainable Food Chain Food Process, Bioprocessing and Food Quality Management, April 18–20, 2011. Nantes, France.
- Zueco, J., Alhama, F., Gonzalez Fernandez, C.F., 2004. Inverse determination of the specific heat of foods. *Journal of Food Engineering* Vol. 64, pp. 347–353.

A. RRS result figures

A.1. 660L PUR Container

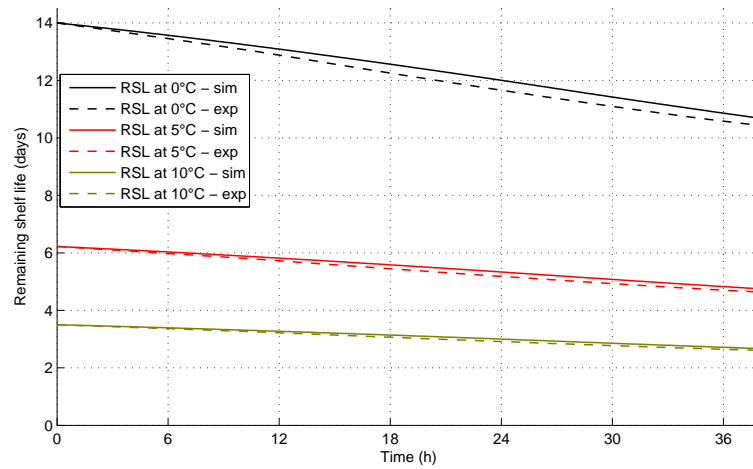


Figure A.1: RRS results at bottom corner in 660 L PUR container.

A. RRS result figures

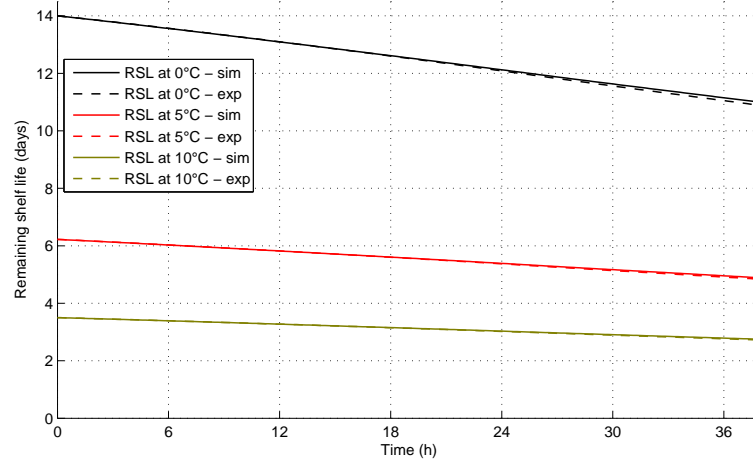


Figure A.2: RRS results at bottom center in 660 L PUR container.

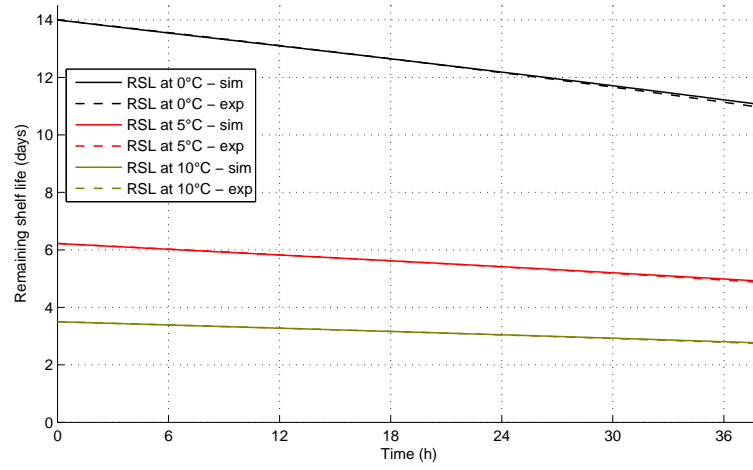


Figure A.3: RRS results at mid center in 660 L PUR container.

A.2. 460L PUR Container

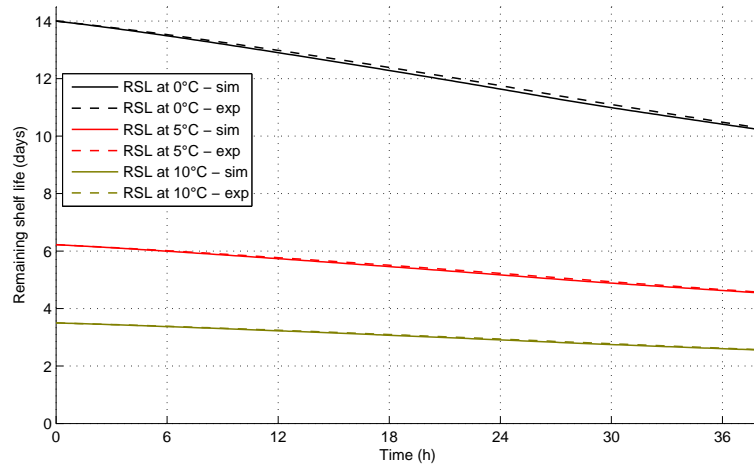


Figure A.4: RRS results at bottom corner in 460 L PUR container.

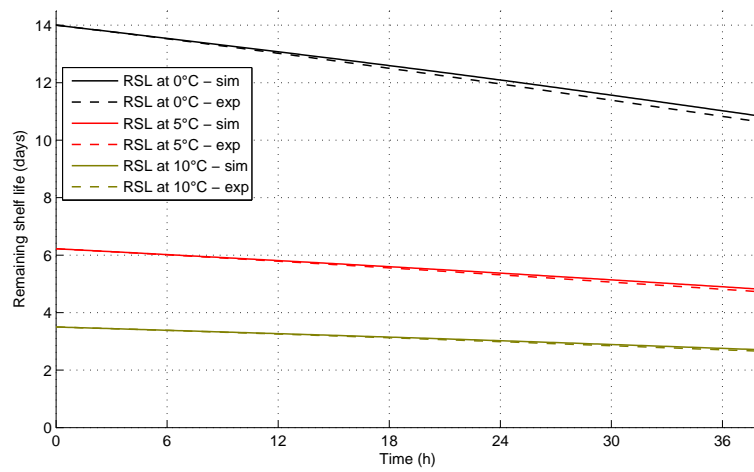


Figure A.5: RRS results at bottom center in 460 L PUR container.

A. RRS result figures

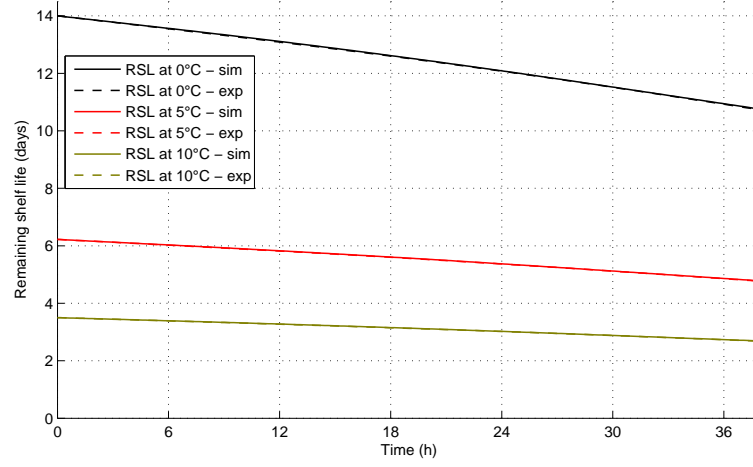


Figure A.6: RRS results at mid center in 460 L PUR container.

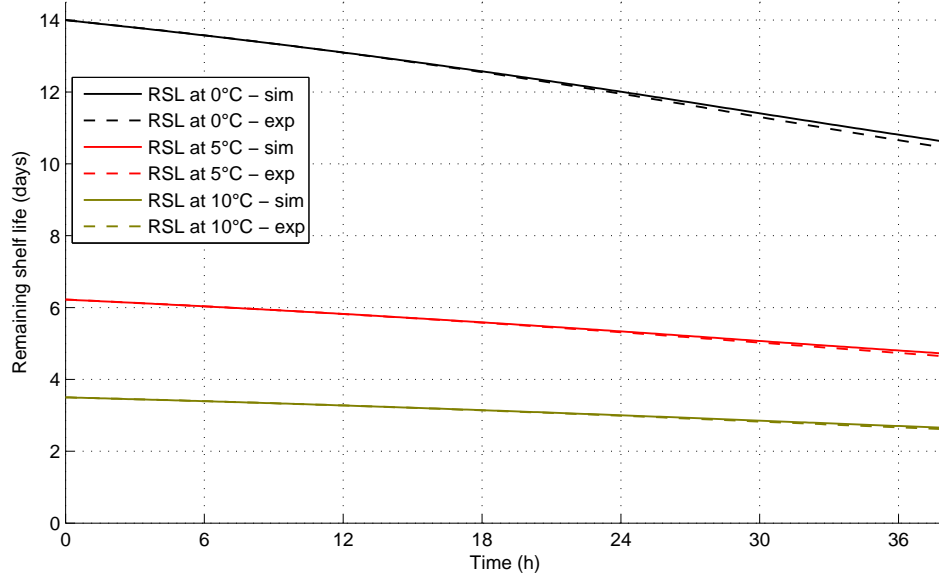


Figure A.7: RRS results at top center in 460 L PUR container.

A.3. 660L PE Container

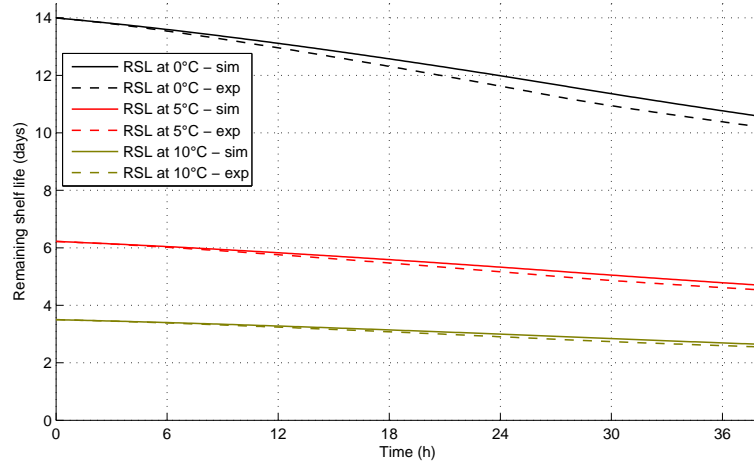


Figure A.8: RRS results at bottom corner in 660 L PE container.

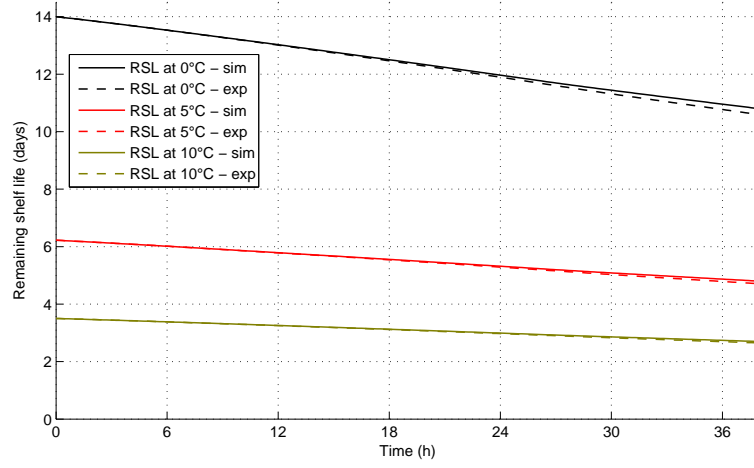


Figure A.9: RRS results at bottom center in 660 L PE container.

A. RRS result figures

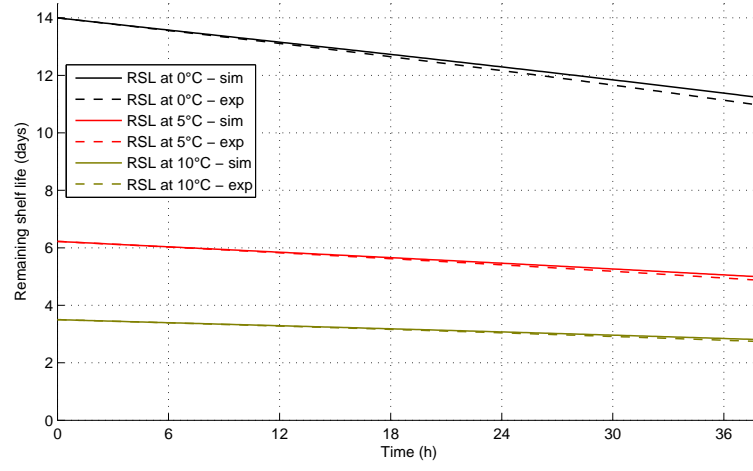


Figure A.10: RRS results at mid center in 660 L PE container.

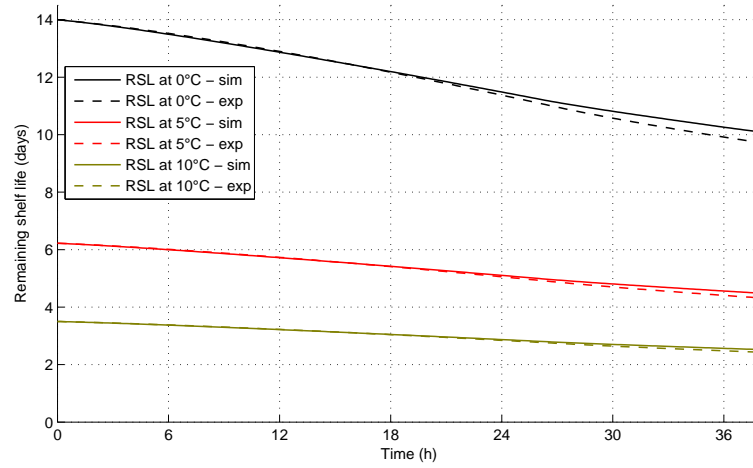


Figure A.11: RRS results at top center in 660 L PE container.

A.4. 460L PE Container

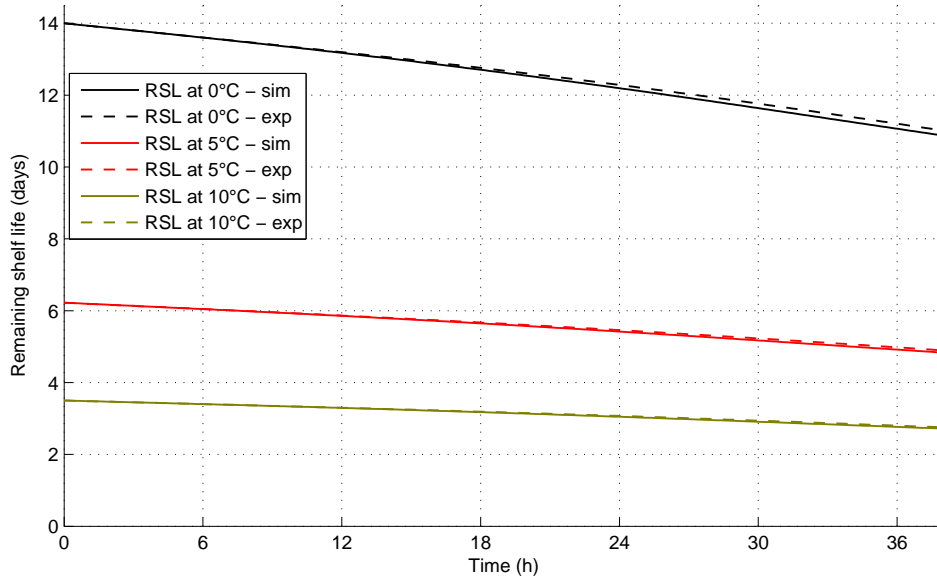


Figure A.12: RRS results at mid center in 460 L PE container.

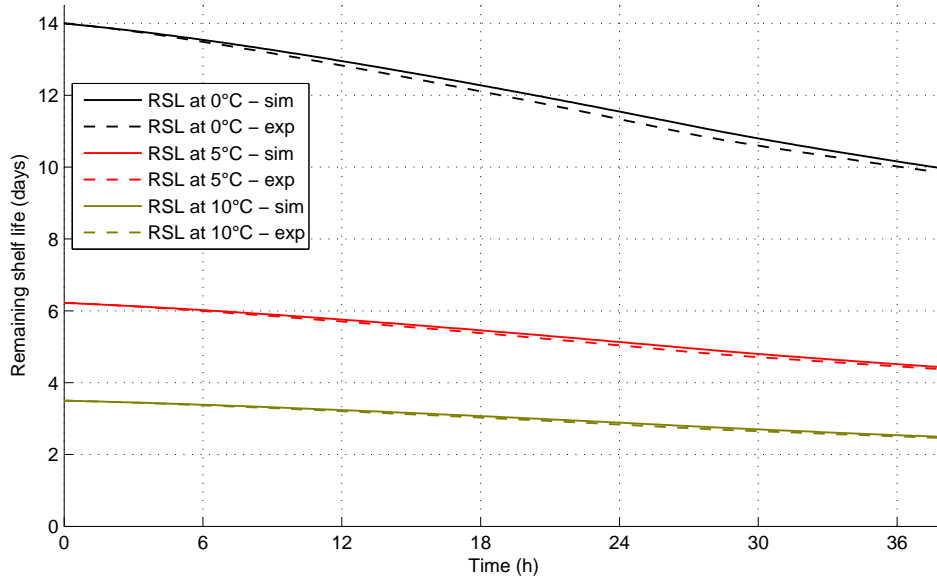


Figure A.13: RRS results at top corner in 460 L PE container.

A. RRS result figures

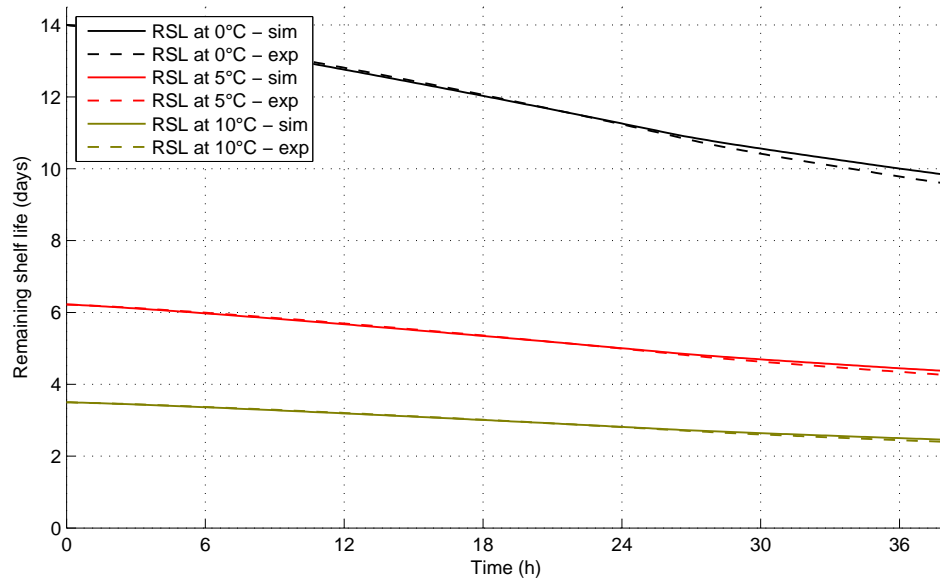


Figure A.14: RRS results at top center in 460 L PE container.

A.5. 340L PE Container

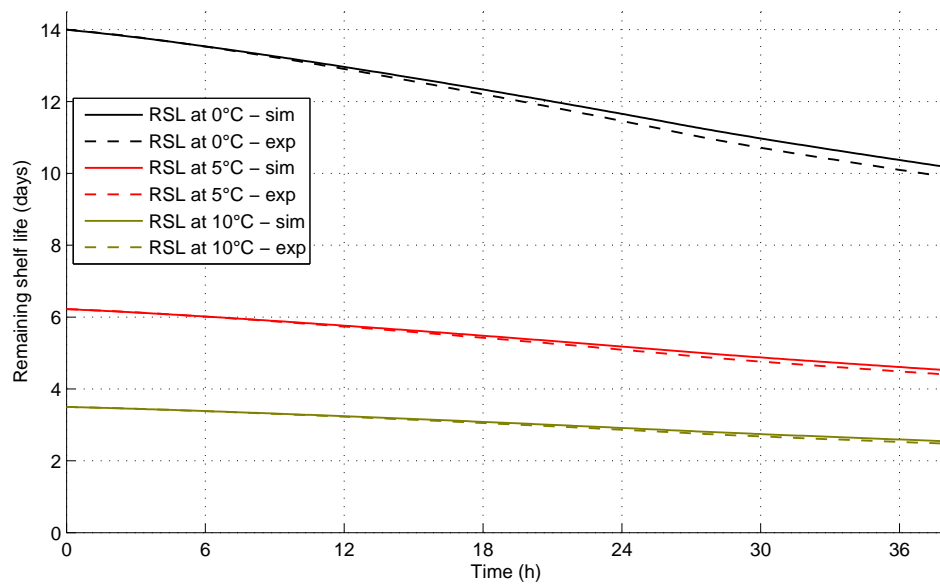


Figure A.15: RRS results at bottom corner in 340 L PE container.

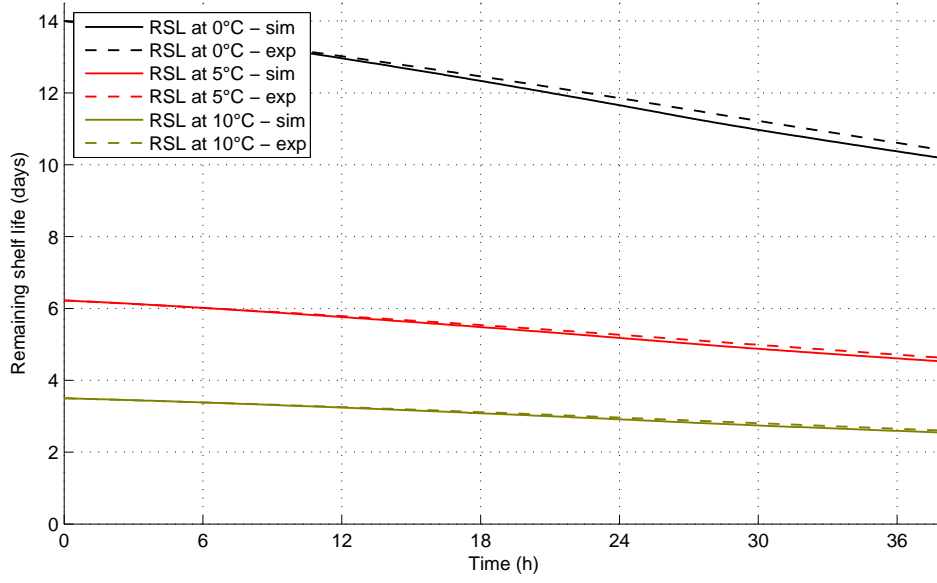


Figure A.16: RRS results at bottom center in 340 L PE container.

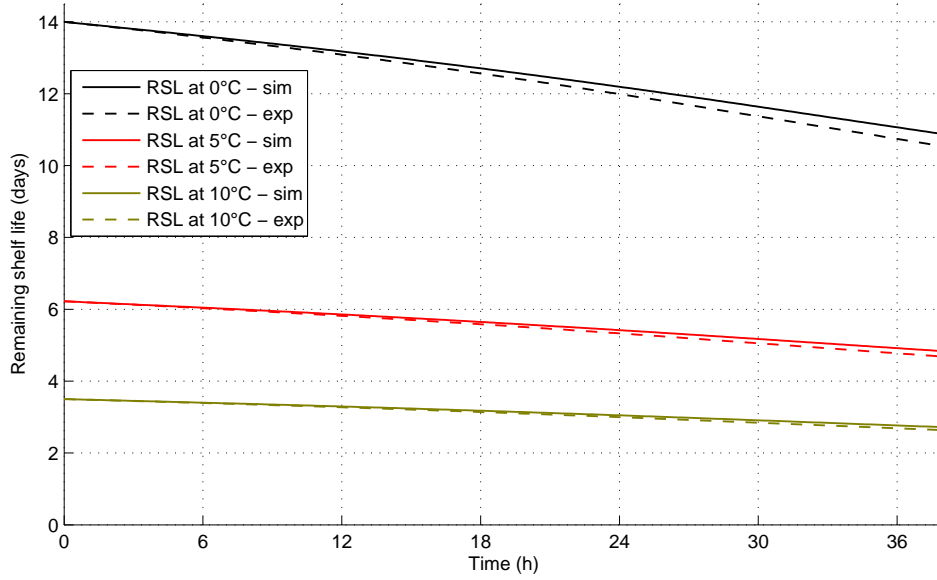


Figure A.17: RRS results at mid center in 340 L PE container.

A. RRS result figures

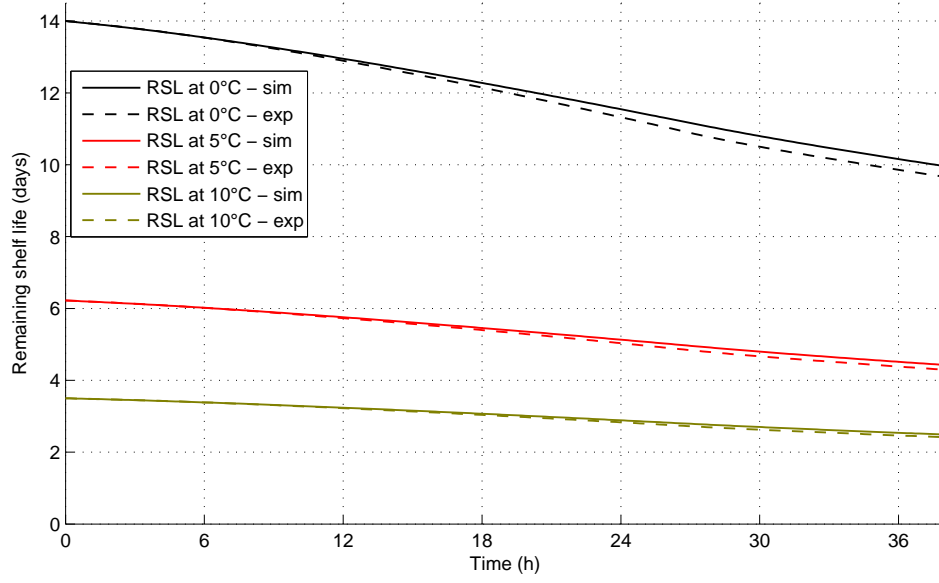


Figure A.18: RRS results at top corner in 340 L PE container.

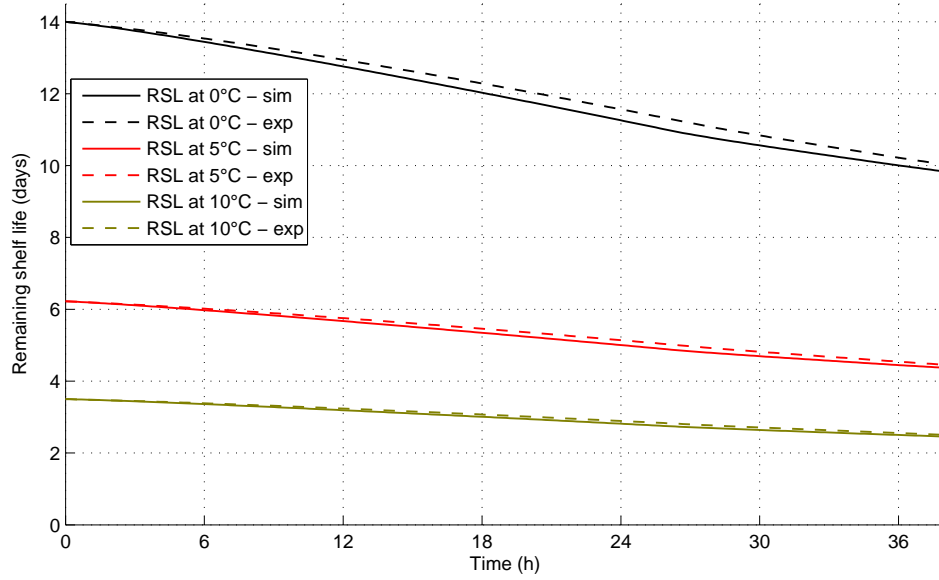


Figure A.19: RRS results at top center in 340 L PE container.